Title: **Genetic risk of dementia modifies obesity effects on white matter myelin in cognitively healthy adults.**

Authors: Jilu P. Mole[1], Fabrizio Fasano[2], John Evans[1], Rebecca Sims[3], Derek A. Hamilton[5], Emma Kidd[6] & Claudia Metzler-Baddeley[1&],

Affiliation: [1]Cardiff University Brain Research Imaging Centre (CUBRIC), School of Psychology, Cardiff University, Maindy Road, Cathays, Cardiff, CF24 4HQ, UK; [2]Siemens Healthcare, Head Office, Sir William Siemens Square, Surrey, GU16 8QD, UK; [3]Division of Psychological Medicine and Clinical Neuroscience, School of Medicine, Cardiff University, Haydn Ellis Building, Maindy Road, Cathays, Cardiff, CF24 4HQ, UK; [4]Department of Psychology, The University of New Mexico, USA. [6]School of Pharmacy and Pharmaceutical Sciences, Cardiff University, Redwood Building, King Edward VII Avenue, Cardiff, CF10 3NB.

[&]Corresponding author:

Claudia Metzler-Baddeley, CUBRIC, Maindy Road, Cardiff CF24 4HQ

Email: Metzler-BaddeleyC@cardiff.ac.uk

Phone: +44 (0)28 2087 0705

Author contributions:

CMB: conceptualization, methodology, formal analysis, writing – original draft preparation, writing – review & editing, visualization, funding acquisition; JPM: investigation, formal analysis, data curation, project administration; RS, EK, DH: Resources; FF, JE: Software.

Disclosure statement: The authors confirm that no financial of non-financial conflicts of interest exist.

Abstract

APOE-ε4 is a major genetic risk factor for late onset Alzheimer's disease (LOAD) that interacts with other risk factors, but the nature of such combined effects remains poorly understood. We quantified the impact of *APOE*-ε4, family history (FH) of dementia, and obesity on white matter (WM) microstructure in 165 asymptomatic adults (38-71 years) using quantitative magnetization transfer (qMT) and Neurite Orientation Dispersion and Density Imaging (NODDI). Microstructural properties of the fornix, parahippocampal cingulum (PHC) and uncinate fasciculus were compared with those in motor and whole-brain WM regions. Widespread interaction effects between *APOE*, FH and Waist-Hip-Ratio were found in the myelin-sensitive macromolecular proton fraction (MPF) from qMT. Amongst individuals with the highest genetic risk (FH+ and *APOE*-ε4) obesity was associated with reduced MPF in the right PHC while no effects were present for those without FH. Risk effects on apparent myelin were moderated by hypertension and inflammation-related markers. These findings suggest that genetic risk modifies the impact of obesity on WM myelin consistent with neuroglia models of aging and LOAD.

2

1. Introduction

As the world's population is aging, increasing numbers of people over 65 will develop cognitive impairment due to late onset Alzheimer's disease (LOAD) (Gulland, 2012). The pathological processes leading to LOAD accumulate over many years (Jack et al., 2013) but it remains challenging to reliably identify those individuals at heightened risk that will develop memory impairments. It is therefore important to gain a better understanding of the effects of dementia risk factors on the brain, and of how they differ from healthy aging. Here we utilized multi-parametric magnetic resonance imaging (MRI) quantification of apparent myelin, cell metabolism, free water, axon density and dispersion to gain information about white matter microstructural differences associated with heightened risk of LOAD. The impact of three main risk factors, *APOE*-ε4 genotype, family history of dementia, and central obesity, on limbic white matter was studied in 165 cognitively healthy individuals from the Cardiff Ageing and Risk of Dementia Study (CARDS) (38 – 71 years) (Table 1) (Coad et al., 2020; Metzler-Baddeley et al., 2019a; Metzler-Baddeley et al., 2019c).

Insert Table 1 here

Accumulating evidence suggests that neuroglia damage may be critically involved in the pathogenesis of LOAD (Bartzokis, 2004; Bartzokis, 2011; De Strooper and Karran, 2016; Heneka, 2017; Nasrabady et al., 2018; Sarlus and Heneka, 2017; Sochocka et al., 2018; Tejera and Heneka, 2016). According to the myelin hypothesis (Bartzokis, 2011; Nasrabady et al., 2018) oligodendrocytes are particularly vulnerable to the impact of aging and insults from genetic and lifestyle risk factors, leading to an accelerated breakdown of axon myelin sheaths with advancing age (Bartzokis, 2004; Bartzokis et al., 2010; Bradl and Lassmann, 2010). Myelin regulates saltatory conduction and synaptic plasticity and is therefore critical for the speed of information transfer and the maintenance of healthy brain circuit functions (Fields, 2014; Fields et al., 2014; Fields and Dutta, 2019; Turner, 2019). When myelin gets

damaged, the brain triggers complex repair mechanisms involving, amongst others, the beta-secretase enzyme BACE1 (Hu et al., 2006; Hu et al., 2017; Nave and Salzer, 2006) that generates amyloid-β (Vassar, 2004). Thus, the myelin model predicts that myelin damage precedes the development of LOAD pathology (Bartzokis, 2011) and consequently, one may expect accelerated myelin damage in individuals at heightened risk of LOAD from midlife onwards (Bartzokis et al., 2010; Flechsig, 1920; Raz, 2001).

APOE is the main cholesterol transporter in the brain (de Chaves and Narayanaswami, 2008) and has three alleles ε2, ε3 and ε4. The *APOE*-ε4 isoform is thought to have fewer molecules to deliver cholesterol required for myelin and synaptic repair (de Chaves and Narayanaswami, 2008; Gong et al., 2002). *APOE*-ε4 is also the largest known genetic risk factor of LOAD with ε4 homozygotes having a 14-fold increase in their lifetime risk compared with ε2 and ε3 carriers (Hersi et al., 2017; Mahoney-Sanchez et al., 2016). It is well-established that *APOE*-ε4 at older age is associated with an earlier onset of LOAD (Filippini et al., 2011; Hersi et al., 2017) and a larger burden of amyloid-β plaques (Chételat and Fouquet, 2013; Gottesman et al., 2016; Kantarci et al., 2012; Lim et al., 2017; Toledo et al., 2019) and this is particularly the case in those individuals with a family history of LOAD (Payami et al., 1997; Yi et al., 2018). Furthermore, *APOE*-ε4 may interact with life-style related risk factors of LOAD, notably central obesity (Beydoun et al., 2008; Pedditizi et al., 2016). Excessive abdominal visceral fat can lead to a metabolic syndrome, type 2 diabetes and cardiovascular disease (Cox et al., 2015), and midlife obesity has been shown to predict the onset of LOAD and neuropathology at autopsy (Chuang et al., 2016). *APOE*-ε4 carriers may be particularly susceptible to the adverse effects of obesity on metabolism and cardiovascular function and show an increased risk of developing hypertension, inflammation and insulin resistance (Ghebranious et al., 2011; Jones and Rebeck, 2018).

There is evidence for *APOE*-ε4, family history and obesity relating to white matter microstructural differences in pathways of the limbic system and those connecting temporal and frontal lobes (Adluru et al., 2014; Kullmann et al., 2015; Lancaster et al., 2016). All three

risk factors are also associated with differences in cognition including episodic memory, spatial navigation, executive functions and processing speed (Alfaro et al., 2018; Aschenbrenner et al., 2016; Bloss et al., 2008; Bondi et al., 1995; Kunz et al., 2015; Loprinzi and Frith, 2018; Luck et al., 2015; O'Donoghue et al., 2018a). For instance, *APOE-ε4* carriers with a parental history of LOAD exhibited white matter microstructural alterations (increased axial diffusivity) in the uncinate fasciculus, a pathway that connects temporal and prefrontal cortices (Adluru et al., 2014). Similarly, baseline white matter microstructural differences in the fornix, the parahippocampal cingulum and the uncinate fasciculus predicted episodic memory decline over three years in asymptomatic older adults enriched with *APOE-ε4* and family history of LOAD (Lancaster et al., 2016). Previously, we have found that central obesity measured with the Waist-Hip-Ratio (WHR) and abdominal visceral fat fractions had adverse effects on fornix microstructure (Metzler-Baddeley et al., 2019a). Accumulating evidence suggests that visceral obesity contributes to deep white matter lesions and cognitive impairments and that these effect may be mediated by neuroinflammation (Lampe et al., 2019; Metzler-Baddeley et al., 2019a; Zhang et al., 2018). Finally, stronger correlations between obesity state and performance in executive function and memory tests were observed in *APOE-ε4* carriers than non-carriers (Zade et al., 2013), suggesting that *APOE* may modulate the effects of obesity on cognition.

These findings point to complex interplays between *APOE-ε4*, family history, and obesity but the nature of these relationships and their underlying mechanisms remain poorly understood. It is generally assumed that *APOE-ε4* combines with family history and obesity to greater impairments in ways that are influenced by age and sex (Bendlin et al., 2010; Jones and Rebeck, 2018; Yi et al., 2018). However, it is also conceivable that a lack of main effects of *APOE-ε4* on white matter microstructure observed in some studies (Bendlin et al., 2010; Dell'Acqua et al., 2015) may be due to counteracting or masking effects of other genetic and/or lifestyle factors and *vice versa.* For instance, there are reports of positive associations between white matter microstructure and central obesity (Birdsill et al., 2017)

as well as serum cholesterol levels (Warstadt et al., 2014) and the question arises whether such apparent protective effects could mask any detrimental effects of *APOE-*ε4 when not controlled for. For these reasons we were interested in modelling main and interaction effects between *APOE,* family history of dementia, and central obesity (assed with WHR) on a number of multi-parametric MRI measurements sensitive to apparent myelin and axon microstructure in white matter.

Insert Figure 1 here

Based on the myelin model, we hypothesized that risk-related interaction effects would be particularly apparent in myelin-sensitive metrics. We therefore went beyond conventional diffusion tensor imaging (Beaulieu and Allen, 1994; De Santis et al., 2014; Pierpaoli and Basser, 1996) and employed more myelin-sensitive indices from quantitative magnetization transfer (qMT) (Cercignani and Alexander, 2006; Eng et al., 1991; Henkelman et al., 1993; Henkelman et al., 2001; Sled, 2018) and T1-relaxometry (Callaghan et al., 2015). The qMT macromolecular proton fraction (MPF) (Sled, 2018), and to a lesser extent the forward exchange rate k_f (Sled, 2018), have been shown highly sensitive to the myelin content in white matter confirmed by histology in Shiverer mice and puppies (Ou et al., 2009a, b; Samsonov et al., 2012; Schmierer et al., 2007; Sled, 2018). MPF has also been reported sensitive to longitudinal myelin changes in Multiple Sclerosis (MS) (Levesque et al., 2010) and to demyelination in MS brains (Schmierer et al., 2007). In addition, widespread reductions in gray matter k_f have been found in LOAD and proposed to reflect impaired cell metabolism (Giulietti et al., 2012) (Figure 1) and the effects of inflammation on the brain (Harrison et al., 2015). Furthermore, the longitudinal relaxation rate R_1 (Callaghan et al., 2015) is a myelin-sensitive measure (Dick et al., 2012; Sereno et al., 2013) that has been associated with LOAD pathology in patients and transgenic mice (for review see (Tang et al., 2018)).

To gain a comprehensive characterisation of white matter microstructure, these myelin-sensitive measurements were complemented by estimates of axon microstructure

from Neurite Orientation Dispersion and Density Imaging (NODDI) (Zhang et al., 2012). NODDI models diffusion-weighted data acquired with two or more b-values to separate free water from hindered and restricted diffusion compartments (Zhang et al., 2012) yielding the isotropic signal fraction (ISOSF) as estimate of free water, the intracellular signal fraction (ICSF) as estimate of apparent axon density, and an axon orientation dispersion index (ODI) (Figure 1). Recent studies in late and early onset AD and transgenic mice suggest that NODDI indices may be sensitive to microstructural degeneration in LOAD (Colgan et al., 2016; Fu et al., 2019; Slattery et al., 2017; Vogt et al., 2019).

Microstructural measurements were derived from the fornix, the parahippocampal cingulum and the uncinate fasciculus as pathways susceptible to synergistic effects of *APOE*-ε4 and family history (Adluru et al., 2014; Lancaster et al., 2016). To assess regional specificity motor cortico-spinal tracts and whole brain white matter masks were included as control areas (Figure 1). Based on the myelin model we predicted risk-related reductions in myelin-sensitive measures of MPF, k_f, and R_1 that may be accompanied by reductions in ICSF and increases in ISOSF and ODI. These microstructural differences were expected to be particularly prominent in the three temporal lobe pathways.

Finally, we also investigated the impact of risk factors on a wide range of cognitive domains including episodic memory (Rey, 1941; Schmidt, 1996), spatial navigation (Hamilton et al., 2002), working memory, executive function, and processing speed (Hampshire et al., 2012; Owen et al., 2010) and tested whether differences in blood pressure, plasma markers of inflammation (C-Reactive Protein, Interleukin 8), and adipose tissue dysfunction (leptin/adiponection ratio) (Frühbeck et al., 2018) moderated any risk effects to explore potential contributing mechanisms.

2. Materials and Methods

The methods of the CARDS study have been previously detailed (Coad et al., 2020; Metzler-Baddeley et al., 2019a; Metzler-Baddeley et al., 2019c) but will be briefly described in the following. CARDS received ethical approval from the School of Psychology Research Ethics Committee at Cardiff University (EC.14.09.09.3843R2) and all participants gave written informed consent.

2.1 Participants

Community-dwelling adults between the age of 35 and 75 years were recruited *via* Cardiff University community panels, notice boards and local poster advertisements. Exclusion criteria of CARDS included a history of neurological and/or psychiatric disease, head injury with loss of consciousness, drug or alcohol dependency, high risk cardio-embolic source or known significant large-vessel disease. All participants had good command of the English language. In total 166 volunteers fulfilled MRI screening criteria and underwent scanning at the Cardiff University Brain Research Imaging Centre. Table 1 summarises details about their demographic background, their cognition, and their genetic and lifestyle risk variables. Participants' intellectual function was assessed with the National Adult Reading Test (NART) (Nelson, 1991), cognitive impairment was screened for with the Mini Mental State Exam (MMSE) (Folstein et al., 1975) and depression with the Patient Health Questionnaire (PHQ-9) (Kroenke et al., 2001).

2.2 Assessment of genetic risk factors

Participants provided saliva samples using the Genotek Oragene-DNA kit (OG-500) for DNA extraction and *APOE* genotyping. *APOE* genotypes ε2, ε3 and ε4 were determined by TaqMan genotyping of single nucleotide polymorphism (SNP) rs7412 and KASP genotyping of SNP rs429358 (Metzler-Baddeley et al., 2019a). Genotyping was successful in 165 of the 166 participants who had an MRI scan. Information about family history of

dementia, i.e. whether a first-grade relative (parent or sibling) was affected by LOAD, vascular dementia or any other type of dementia was provided by self-report.

2.3 Assessment of metabolic syndrome-related risk factors

Participants' waist and hip circumferences and their resting systolic and diastolic blood pressure (BP) were measured. Central obesity was defined as a WHR ≥ 0.9 for males and ≥ 0.85 for females and hypertension as systolic BP ≥ 140 mm Hg. Other metabolic risk factors, such as diabetes mellitus, statin medication, history of smoking, and weekly alcohol intake were self-reported in a medical history questionnaire (Metzler-Baddeley et al., 2013) (Table 1). As there were relatively few diabetics, smokers, and individuals on statins these variables were not included in the statistical analyses (Table 1).

2.4 Blood plasma analysis

As previously reported (Metzler-Baddeley et al., 2019a), venous blood samples were drawn into 9ml heparin coated plasma tubes after 12 hours overnight fasting and were centrifuged for 10 minutes at 2,000xg within 1 hour from blood collection. Plasma samples were then transferred into 0.5 ml polypropylene microtubes and stored in a freezer at -80°C. Circulating levels of high-sensitivity C-Reactive Protein (CRP) in mg/dL were assayed using a human CRP Quantikine enzyme-linked immunosorbent assay (ELISA) kit (R & D Systems, Minneapolis, USA). Six individuals had a CRP value > 10 mg/ml indicative of acute infection and were therefore excluded from analyses testing for moderating effects of inflammation. Leptin concentrations in pg/ml were determined with the DRP300 Quantikine ELISA kit (R & D Systems) and adiponectin in ng/ml with the human total adiponectin/Acrp30 Quantitkine ELISA kit (R & D Systems). Leptin/adiponectin ratios for each participant were calculated. Interleukin IL-8 levels in pg/mL were determined using a high sensitivity CXCL8/ INTERLEUKIN-8 Quantikine ELISA kit (R & D Systems). Determination of interleukin-1β, interleukin-6 and Tumor Necrosis Factor α (TNFα) levels were trialled with high-sensitivity

Quantikine ELISA kits but did not result in reliable measurements consistently above the level of detection for each assay.

2.5 Cognitive assessment

Details of the cognitive assessment can be found in Coad et al (2020). Verbal and visual recall were assessed with the Rey Auditory Verbal Learning Test (RAVLT) and the complex Rey figure (Rey, 1941; Schmidt, 1996). Short-term topographical memory was measured with the Four Mountains Test (Chan et al., 2016). Spatial navigation was assessed with a virtual Morris Water Maze Task (vMWMT) (Hamilton et al., 2002) that required participants to find and navigate to a hidden platform in a water pool. This task also included a motor control condition, where participants navigated to a visible platform. Working memory capacity and executive functions were assessed with computerised tests from the Cambridge Brain Sciences battery (Hampshire et al., 2012; Owen et al., 2010) and included the following: digit and spatial span, a version of the Stroop test (Double-Trouble), problem solving with a version of the Tower of London task (the Tree task), abstract reasoning with grammatical reasoning and odd-one-out, the ability to manipulate and organize spatial information with a self-ordered spatial span task, intra- and extradimensional shift, choice-reaction time, and object-location paired-associate learning (PAL). Cognitive outcome measures were the number of correct responses and response latencies.

2.6 MRI data acquisition

MRI data were collected on a 3T MAGNETOM Prisma clinical scanner (Siemens Healthcare, Erlangen, Germany) (Metzler-Baddeley et al., 2019a,b). A three-dimension (3D) magnetization-prepared rapid gradient-echo (MP-RAGE) sequence (256 x 256 acquisition matrix, TR = 2300 ms, TE = 3.06 ms, TI = 850ms, flip angle θ = 9°, 176 slices, 1mm slice thickness, FOV = 256 mm and acquisition time of ~ 6 min) was used to acquire T_1-weighted anatomical images.

Diffusion-weighted images were acquired with High Angular Resolution Diffusion Imaging (HARDI) (Tuch et al., 2002) using a spin-echo echo-planar dual shell HARDI sequence with diffusion encoded along 90 isotropically distributed orientations (Jones et al., 1999) (30 directions at b-value = 1200 s/mm^2, 60 directions at b-value = 2400 s/mm^2) and six non-diffusion weighted scans with dynamic field correction (TR = 9400ms, TE = 67ms, 80 slices, 2 mm slice thickness, 2 x 2 x 2 mm voxel, FOV = 256 x 256 x 160 mm, GRAPPA acceleration factor = 2, acquisition time of ~15 min).

An optimized 3D MT-weighted gradient-recalled-echo sequence (Cercignani and Alexander, 2006) was used to collect the quantitative magnetization transfer weighted imaging data with the following parameters: TR = 32 ms, TE = 2.46 ms; Gaussian MT pulses, duration t = 12.8 ms; FA = 5°; FOV = 24 cm, 2.5 x 2.5 x 2.5 mm^3 resolution. Cramer-Rao lower bound optimization was used to optimize the following off-resonance irradiation frequencies (Θ) and their corresponding saturation pulse nominal flip angles (ΔSAT) for the 11 MT-weighted images: Θ = [1000 Hz, 1000 Hz, 2750 Hz, 2768 Hz, 2790 Hz, 2890 Hz, 1000 Hz, 1000 Hz, 12060 Hz, 47180 Hz, 56360 Hz] and their corresponding ΔSAT values = [332°, 333°, 628°, 628°, 628°, 628°, 628°, 628°, 628°, 628°, 332°]. The longitudinal relaxation time, T_1, of the system was estimated by acquiring three 3D gradient recalled echo sequence (GRE) volumes with three different flip angles (θ = 3°,7°,15°). This was done with the same acquisition parameters as used in the MT-weighted sequence (TR = 32 ms, TE = 2.46 ms, FOV = 24 cm, 2.5 x 2.5 x 2.5 mm^3 resolution). Finally, data for computing the static magnetic field (B_0) were collected using two 3D GRE volumes with different echo-times (TE = 4.92 ms and 7.38 ms respectively; TR= 330ms; FOV= 240 mm; slice thickness 2.5 mm) (Jezzard and Balaban, 1995).

2.7 HARDI and qMT data processing

Microstructural data processing has been detailed in Metzler-Baddeley et al. (2019a,b). The dual-shell HARDI data were split and b = 1200 and 2400 s/mm^2 data were corrected separately for distortions induced by the diffusion-weighted gradients and motion

artefacts with appropriate reorientation of the encoding vectors (Leemans and Jones, 2009) in ExploreDTI (Version 4.8.3) (Leemans A et al., 2009). EPI-induced geometrical distortions were corrected by warping the diffusion-weighted image volumes to the T_1-weighted images (Irfanoglu et al., 2012). Subsequently, the NODDI model (Zhang et al., 2012) was fit to the HARDI data with the fast, linear model fitting algorithms of the Accelerated Microstructure Imaging via Convex Optimization (AMICO) framework (Daducci et al., 2015). By modelling the dual-shell (b = 1200 and 2400 s/mm^2) HARDI data, NODDI allowed the separation of free water contributions to the diffusion signal from hindered and restricted diffusion compartments (Zhang et al., 2012) to calculate isotropic signal fraction (ISOSF), intracellular signal fraction (ICSF), and orientation dispersion index (ODI) maps.

The qMT method models the exchange rate between macromolecular protons and protons in surrounding free water when macromolecular protons are selectively saturated by a radiofrequency pulse with a frequency that is off-resonance for protons in free water (Cercignani and Alexander, 2006; Eng et al., 1991; Henkelman et al., 1993; Henkelman et al., 2001; Sled, 2018). MT-weighted GRE volumes were co-registered to the MT-volume with the most contrast using a rigid body (6 degrees of freedom) registration to correct for inter-scan motion using Elastix (Klein et al., 2010). Data from the 11 MT-weighted GRE images and T_1-maps were fit by the two-pool Ramani pulsed-MT approximation model (Ramani et al., 2002). This approximation provided MPF, k_f and R_1 maps. MPF maps were thresholded to an upper intensity limit of 0.3 and k_f maps to an upper limit of 3.0 using the FMRIB's fslmaths imaging calculator to remove voxels with noise-only data.

All parametric maps and region of interest masks were spatially aligned to the T_1-weighted anatomical volume in within-subject space with linear affine registration (12 degrees of freedom) using FMRIB's Linear Image Registration Tool (FLIRT) (Jenkinson et al., 2012).

2.8 Tractography

As previously reported (Metzler-Baddeley et al., 2019a,b), the RESDORE algorithm (Parker, 2014) was applied to identify outliers and whole brain tractography with the damped

Richardson-Lucy algorithm (dRL) (Dell'acqua et al., 2010) was carried out on the 60 direction, $b = 2400$ s/mm² HARDI data for each dataset in single-subject space using in house software (Parker, 2014) coded in MATLAB (the MathWorks, Natick, MA). To reconstruct fibre tracts, dRL fibre orientation density functions (fODFs) were estimated at the centre of each image voxel with seed points positioned at the vertices of a 2x2x2 mm grid superimposed over the image. The tracking algorithm interpolated local fODF estimates at each seed point and then propagated 0.5mm along orientations of each fODF lobe above a threshold on peak amplitude of 0.05. Individual streamlines were subsequently propagated by interpolating the fODF at their new location and propagating 0.5mm along the minimally subtending fODF peak. This process was repeated until the minimally subtending peak magnitude fell below 0.05 or the change of direction between successive 0.5mm steps exceeded an angle of 45°. Tracking was then repeated in the opposite direction from the initial seed point. Streamlines whose lengths were outside a range of 10mm to 500mm were discarded.

The fornix, parahippocampal cinguli (PHC), uncinate fasciculus (UF) and corticospinal (CST) pathways were reconstructed with an in-house automated segmentation method based on principal component analysis (PCA) of streamline shape (Parker et al., 2012). This procedure involves the manual reconstruction of a set of tracts that are then used to train a PCA model of candidate streamline shape and location. Twenty datasets were randomly selected as training data. Tracts were reconstructed by manually applying waypoint region of interest (ROI) gates ("AND", "OR" and "NOT" gates following Boolean logic) to isolate specific tracts from the whole brain tractography data. ROIs were placed in HARDI data native space on color-coded fiber orientation maps (Pajevic and Pierpaoli, 1999) in ExploreDTI following previously published protocols (Metzler-Baddeley et al., 2013; Metzler-Baddeley et al., 2012a; Metzler-Baddeley et al., 2011; Metzler-Baddeley et al., 2012b). The trained PCA shape models were then applied to all datasets: candidate streamlines were selected from the whole volume tractography as those bridging the gap between estimated end points of the candidate tracts. Spurious streamlines were excluded by means of a shape comparison with the trained PCA model. All automatic tract reconstructions underwent quality control through visual inspection

and any remaining spurious fibers that were not consistent with the tract anatomy were removed from the reconstruction where necessary. Mean values of all qMT and NODDI indices were extracted for all white matter pathways.

2.9 Whole brain white matter segmentation

Whole brain white matter masks were automatically segmented from T_1- weighted images with the Freesurfer image analysis suite (version 5.3), which is documented online (https://surfer.nmr.mgh.harvard.edu/). Whole brain white matter masks were thresholded to exclude ventricular cerebrospinal fluid spaces from the mask. Mean values of all qMT and NODDI indices were extracted for the whole brain white matter mask. This was done by loading each participants' microstructural maps on his/her whole brain white matter mask using the fslmaths command from the FMRIB Software Library v6.0 (Jenkinson et al., 2012) and then calculating the mean microstructural value from all voxels within the whole brain white matter mask with the fslstats command.

2.10 Statistical analysis

Statistical analyses were conducted in SPSS version 20 (IBM, 2011). All microstructural data were examined for outliers defined as above or below three times the interquartile range (75th percentile value - 25th percentile value) to fulfil assumptions of normal distribution and variance homogeneity of parametric testing. This led to an exclusion of 2.3% of the microstructural and 2.4% of the cognitive data.

A full-factorial linear multivariate analysis of covariance (MANCOVA) that modelled the main effects of *APOE* genotype (ε4+, ε4-), FH (FH+, FH-) and obesity (WHR+, WHR-) as well as any two-way and three-way interaction terms (i.e. *APOE**WHR, *APOE**FH, WHR*FH, *APOE**FH*WHR) on all microstructural indices (MPF, k_f, R_1, ISOSF, ICSF, ODI) in all white matter pathways (left PHC, right PHC, left UF, right UF, left CST, right CST and fornix) and the WBWM region was employed. The same MANCOVA was carried out to test for effects on all cognitive factors (see below). These analyses were controlled for age, sex and NART-

IQ as these variables are known to influence LOAD risk (Altmann et al., 2014; Damoiseaux et al., 2012). A False Discovery Rate (FDR) of 5% using the Benjamini-Hochberg procedure (Benjamini and Hochberg, 1995) (p_{BHadj}) was applied to all primary and post-hoc models to account for multiplicity of testing (Cramer et al., 2016). Information about effects sizes was provided with partial eta squared η_p^2, r and R^2 indices. All reported p-values were two-tailed.

The dimensionality of the cognitive data was reduced with exploratory factor analyses (EFA) with unweighted least squares and orthogonal varimax rotation with a maximum of 5000 iterations for conversion (Coad et al., 2020). Variables with communalities < 0.4 were excluded from the final EFA (Osborne et al., 2008). After inspection of Cattell's scree plot (Cattell, 1952), factors with an eigenvalue exceeding 2 were extracted and factor loadings exceeding 0.5 were considered for the interpretation of the factors. The resulting cognitive factors were then entered as dependent variables into the above described MANCOVA model. Finally, Pearson correlation coefficients were calculated to explore relationships between white matter microstructure and cognition.

3. Results

3.1 Participant characteristics

There were 166 participants between the ages of 38 and 71 years (Mean = 55.8, SD = 8.2) (94 females) who underwent MRI scanning. CARDS participants as a group were of above average intelligence (Table 1) and were cognitively healthy with the exception of one individual with a MMSE score of 26, who was excluded from the analysis (n = 165). Eight participants scored ≥ 10 in the PHQ-9 suggesting moderate levels of depression but no participant was severely depressed. Two participants reported high levels of weekly alcohol consumption (42 and 60 units).

Sixty-four individuals were *APOE*-ε4 carriers (7 homozygotes), 69 reported a family history (FH) of dementia and 103 were centrally obese. Only three individuals reported being

diabetic. The frequency of *APOE*-ε4 carriers in CARDS was 36%, which is higher than expected in the normal population (15-20%). We propose that this may reflect a recruitment bias as volunteers in dementia research are more likely to have a family history of disease and therefore an increased *APOE*-ε4 frequency. Having said this the proportion of *APOE*-ε4 carriers did not differ between individuals with or without FH (p = 0.2) [30.5% (n = 18) for FH+ versus 43% (n = 46) for FH-]. There were no significant differences in WHR between *APOE*-ε4 carriers and non-carriers (p = 0.35) or between individuals with and without FH (p = 0.9). Groups were comparable with regards to age (APOE: p = 0.7, FH: p = 0.05, WHR: p = 0.07) and NART-IQ (APOE: p = 0.8, FH: p = 0.8, WHR: p = 0.5) although there were trends for individuals with FH and central obesity to be slightly older. The FH groups were comparable with regards to the distribution of sex (56% FH+ females, 57% FH- females). *APOE*-ε4 carriers had an equal distribution of men and women (50%) but there were more women amongst non-carriers (61%). More men than women were centrally obese (41% females) and more women than men had a normal WHR (83% females). Neither *APOE* or FH groups showed differences in systolic blood BP (*APOE*: p = 0.7, FH = 0.3), diastolic BP (*APOE*: p = 0.6, FH: p = 0.9), CRP (*APOE*: p = 0.2, FH: p = 0.98), IL-8 (*APOE*: p = 0.6, FH: p = 0.8) or in the leptin/adiponectin ratio (*APOE*: p = 0.2, FH: p = 0.9). Centrally obese relative to normal individuals had higher diastolic BP [t(164) = 2.6, p = 0.01] with a trend for higher systolic BP (p = 0.07) and had a lower leptin/adiponectin ratio [t(146) = 2.3, p = 0.02]. They did not differ in CRP (p = 0.5) or IL-8 levels (p = 0.6).

Insert Table 2 and Figure 2 here

3.2 Multivariate covariance analysis (MANCOVA) of white matter microstructural indices

MANCOVA tested for the effects of *APOE* genotype (ε4+, ε4-), family history (FH+, FH-) and central obesity (WHR+, WHR-) on all microstructural indices (MPF, k_f, R_1, ISOSF,

ICSF, ODI) in all white matter pathways (left PHC, right PHC, left UF, right UF, left CST, right CST and fornix) and WBWM regions whilst controlling for age, sex and NART-IQ.

$Omnibus$ $effects$: Main effects were observed for age [$F_{(48,60)}$ = 2.4, p_{BHadj} = 0.005, η_p^2 = 0.66] and sex [$F_{(48,60)}$ = 2.7, p_{BHadj} < 0.001, η_p^2 = 0.68]. A three-way interaction effect was present between $APOE$, FH and WHR [$F_{(48,60)}$ = 1.8, p_{BHadj} = 0.04, η_p^2 = 0.6].

$Post$-hoc $effects$: Ageing was associated with reductions in MPF, k_f, and R_1 in WBWM, fornix and right UF (Table 2). MPF and k_f reductions were also present in the left UF and reductions in k_f in bilateral CST. In addition, age-related increases in ISOSF were observed in the fornix and WBWM (Table 2, Figure 2A). Women relative to men showed higher MPF and lower ISOSF in the fornix and lower k_f and ISOSF in WBWM (Table 2, Figure 2B).

Three-way interaction effects between FH, $APOE$ and WHR were observed for MPF in WBWM, bilateral CST, bilateral UF and right PHC (Figure 3B). For right PHC there was also an effect on ICSF. These three-way interaction effects were followed up by testing for $APOE$ and WHR interactions in FH+ and FH- individuals separately (Figure 3C). FH-individuals did not show an omnibus interaction effects between $APOE$ and WHR [$F_{(7,88)}$ = 0.9, p_{BHadj} = 0.05]. In contrast, FH+ individuals exhibited a significant omnibus $APOE$ x WHR interaction effect [$F_{(7,45)}$ = 4.3, p_{BHadj} = 0.002, η_p^2 = 0.4] due to the following pattern: For $APOE$-ε4+ carriers, centrally obese relative to normal individuals had lower MPF and ICSF in the right PHC. The opposite pattern was observed for non-carriers with obese relative to normal individuals showing larger MPF in the right PHC (Table 2, Figure 3C).

3.3 Effects of vascular and inflammation-related moderators

We then explored with two separate MANCOVAs whether controlling for differences in i) cardiovascular measures of systolic and diastolic BP as well as BP medication and ii) inflammation-related measures of CRP, IL-8 and leptin/adiponectin ratio would account for

the three-way interaction effects on MPF in WBWM, bilateral CST, bilateral UF and right PHC and right PHC ICSF.

There was a main effect of systolic BP [$F(7,135) = 4.7$, $p_{BHadj} < 0.001$, $\eta_p^2 = 0.19$] with systolic BP correlating negatively with WBWM MPF ($r = -0.22$, $p_{BHadj} = 0.01$). After the inclusion of BP covariates there was only a trend for the interaction effect between *APOE*, FH and WHR ($p_{BHadj} = 0.07$). No significant main effects were observed for CRP, IL-8 and leptin/adiponectin ratio but accounting for these variables removed the interaction effect between *APOE*, FH and WHR ($p_{BHadj} = 0.54$).

3.4 Exploratory Factor Analysis of cognitive scores

Exploratory Factor Analysis (EFA) reduced the dimensionality of the cognitive data to seven factors, explaining together 49% of the variance in cognition (see Table 3 in Coad et al 2020). The first factor captured "Verbal Recall" with high loadings on the Rey Auditory Verbal Learning Test (RAVLT). The second factor captured elements of "Motor planning and speed" with high loadings on first move latencies in all conditions of the vMWMT and of total latencies in the motor control condition in the vMWMT. A third factor captured "Spatial Navigation" behaviour with high loadings on path lengths and total latencies in the hidden platform condition of the vMWMT. The fourth factor captured "Attention Set" with high loadings on the intra-dimensional subcomponents of the an intra- and extradimensional (IDED) attention set task. The fifth factor captured "Visuospatial Memory" with loadings on immediate and delayed recall of the Rey Complex Figure and the Spatial Span task. The sixth factor captured "Working Memory" capacity due to loadings on Digit Span and Spatial Search. Finally, the seventh "Paired Associated Learning" factor had high loadings on an object object-location paired associate learning task.

3.5 MANCOVA of cognitive measurements

MANCOVA testing for the effects of *APOE* genotype, FH and WHR on the seven cognitive factors were carried out while controlling for age, sex and NART-IQ.

Omnibus effects: There was a main effect of age [$F(7,105) = 5.9$, $p_{BHadj} < 0.001$, $\eta_p^2 = 0.28$]. A trend for an omnibus interaction effect between FH and WHR was observed ($p_{BHadj} = 0.08$).

Post-hoc effects: Age had significant effect on the "Motor Speed and Planning" factor [$F(1,111) = 14.7$, $p_{BHadj} < 0.001$, $\eta_p^2 = 0.15$] reflecting a slowing of response latencies with age ($r_{Age\text{-}MotorSpeed} = 0.37$, $p < 0.001$).

3.6 Relationship between motor speed and white matter myelin

To test the hypothesis that age-related differences in apparent white matter myelin were underpinning age-related response slowing, Pearson correlation coefficient was calculated between differences in "Motor Speed and Planning" and differences in WBWM MPF followed by a partial correlation controlling for age. There was a negative correlation between "Motor Speed and Planning" and WBWM MPF ($r = -0.23$, $p = 0.015$) which was removed when controlling for age ($r = -0.1$, $p = 0.3$).

4. Discussion

The strength of the present study consisted in utilizing advanced multi-parametric MRI quantifications of white matter microstructure to investigate combined effects of *APOE-ε4* genotype, family history of dementia, and central obesity on brain microstructure in 165 cognitive healthy adults. Quantitative indices from qMT, relaxometry and NODDI sensitive to apparent myelin, cell metabolism, free water, axon density and dispersion were employed to provide information about white matter differences due to heightened dementia risk. This approach also allowed us to dissociate risk-specific effects on white matter microstructure from those due to aging and sex.

We observed no main effects but widespread three-way interactions between *APOE,* FH and WHR in the macromolecular proton fraction MPF from qMT. These effects were most prominent in the right PHC. MPF has been found highly sensitive to white matter myelin in combined imaging and histology Shiverer studies (Ou et al., 2009a, b; Samsonov et al., 2012; Schmierer et al., 2007; Sled, 2018). No risk effects though were observed on k_f, R_1, ISOSF, or ODI. Furthermore, ICSF, a measure of apparent axon density, was only affected in the right PHC but not in any other white matter regions. As MPF was considered the most sensitive index for white matter myelin, these findings suggest that *APOE*, FH and central obesity were primarily associated with differences in white matter myelin rather than cell metabolism, axon microstructure or free water. These findings are consistent with the myelin model (Bartzokis, 2011) that proposes adverse effects of aging and risk on myelin sheaths preceding the development of LOAD pathology.

In contrast to white matter microstructure we did not find any effects of risk factors on cognition although a trend for an interaction between FH and WHR was observed. As it has been recognised that impaired cognition in older adults at heightened risk may arise from early LOAD pathology (O'Donoghue et al., 2018b), it is possible that CARDS participants were too young to have developed any significant pathology to affect cognition. Instead we propose that the risk-related differences in apparent myelin may reflect very early

vulnerabilities that precede LOAD pathology and do not affect cognition in asymptomatic individuals yet. On the other hand, it is also possible that our cognitive measures were not sufficiently sensitive to reveal subtle cognitive differences between the risk groups (O'Donoghue et al., 2018b). In this context it is noteworthy that post-hoc exploration of the FH and WHR interaction trend revealed a potential impact on the Spatial Navigation factor that would be interesting to pursue further in future studies.

Post-hoc analyses of the three-way interaction risk effect revealed that effects between *APOE* and WHR were dependent on an individual's family history state. For those individuals with the highest genetic risk, based on *APOE*-ε4 and a positive family history of dementia, obesity was associated with lower MPF and ICSF in the right PHC, whilst *APOE*-ε2 and ε3 carriers with a positive family history showed the opposite effect, i.e. larger MPF in obese compared to non-obese individuals. Meanwhile *APOE* or WHR had no effect in those individuals without a family history of dementia.

The PHC connects the posterior cingulate and parietal cortices with the medial temporal lobes (Bubb et al., 2018). Reductions in glucose metabolism and blood oxygen-level dependent signal in these regions have been reported in young and middle-aged *APOE*-ε4 carriers and in LOAD (Chételat and Fouquet, 2013; Reiman et al., 2004). Parahippocampal white matter volume has also been found a sensitive predictor of LOAD in cognitively normal people (Stoub et al., 2014). Recently, Chen et al. (2015) applied graph-based network analysis and revealed reduced global efficiency and functional connectivity in white matter networks as well as reduced functional connectivity in medial temporal lobe regions in older asymptomatic *APOE*-ε4 carriers (Chen et al., 2015). In this study the right parahippocampal gyrus (rPHG) was the only brain region that showed simultaneous functional and structural dysconnectivity, and node efficiency in rPHG mediated *APOE*-ε4-related effects on delayed recall (Chen et al., 2015). Our study provides novel evidence for risk-related myelin vulnerabilities in the right PHC, a pathway that connects those cortical regions with functional abnormalities in *APOE*-ε4 and LOAD.

These risk-specific effects contrasted with age- and sex-related microstructural differences. Aging was not only associated with widespread reductions in MPF but also with reductions in k_f and in R_1 as well as with increases in ISOSF while no effects were observed on ICSF and ODI (Metzler-Baddeley et al., 2019b). These effects were present in most white matter regions except in the PHC and were particularly prominent in the fornix tract. This pattern suggests widespread age-related white matter atrophy (ISOSF) primarily due to a loss of myelin (MPF, R_1) rather than axons (ICSF, ODI) and an age-related slowing of cell metabolism (k_f). Reductions in k_f are consistent with findings of compromised metabolic states related to energy synthesis and oxidative stress in the aging brain (Gaignard et al., 2017; Mattson and Arumugam, 2018) and accord with a recent report of age-related changes in brain metabolites including decreases in N-acetylaspartate (NAA) concentrations (Maghsudi et al., 2019).

The observed aging pattern (Coad et al., 2020; Metzler-Baddeley et al., 2019b) is also consistent with a post-mortem study of rhesus monkeys, that found age-related differences in myelin sheaths and a loss of myelinated but not of unmyelinated axons (Peters et al., 2010). These findings accord with imaging findings indicating that fornix maturation peaks in late adolescence with subsequent volume reductions in healthy ageing that partly reflect a loss of myelinated fibers (Amaral et al., 2018; Douet and Chang, 2014). The overall conclusion from present and previous research is that myelinated white matter fibers are particularly sensitive to aging and risk factors consistent with the myelin model. Our study also provides further evidence for the view that age-related reductions in myelin may underpin response slowing (Bartzokis, 2004; Salthouse, 1976). Besides reductions in apparent white matter myelin, aging was associated with slowing in the motor speed and planning factor. In addition, this factor correlated negatively with whole brain white matter MPF and this correlation was removed when age was controlled for.

With regards to sex we found that women compared with men had higher MPF and lower ISOSF in the fornix and lower ISOSF and k_f in WBWM. In the CARDS cohort women were less obese, had lower systolic BP, and reported drinking less alcohol than men

(Metzler-Baddeley et al., 2019a). All of these factors may have contributed to women showing "healthier" white matter microstructure in terms of larger apparent myelin and less free water contamination. In addition, sex-related differences in k_f may reflect differences in brain mitochondrial function related to oxidative stress between men and women (Gaignard et al., 2018; Gaignard et al., 2015)

It might be noteworthy that we observed anatomical dissociations between genetic risk- and age/sex-effects. Risk interactions on MPF were most prominent in the right PHC but absent in the fornix. In contrast, age and sex effects were strongest in the fornix but absent in the PHC. Thus, genetic risk factor (*APOE* and family history) had an impact on medial temporal lobe input (PHC) but not output (fornix) structures, whilst age and sex as well as obesity (Metzler-Baddeley et al., 2019a) affected output (fornix) but not input (PHC) structures. As *APOE* and family history are associated with earlier and larger amyloid and tau burden (Ossenkoppele et al., 2016; Yi et al., 2018), and LOAD pathology is known to spread from the entorhinal cortices and parahippocampal gyrus into the medial temporal lobes (Braak and Del Trecidi, 2015; Braak and Del Tredici, 2015), these findings might reflect tissue vulnerabilities that may precede the development of LOAD pathology.

It is also noteworthy that, in contrast to age and sex, we did not observe any main effects of risk on white matter microstructure. This pattern of results suggests complex interplays between an individual's genetic make-up and obesity. Besides *APOE* genotype, genome wide association studies (GWAS) have identified a number of genetic risk loci for LOAD, involved in immunity, lipid metabolism as well as tau binding and amyloid precursor protein processing (Kunkle et al., 2019). As self-report of parental history of dementia is likely to represent the presence of some of these genetic risk variants (Marioni et al., 2018), our effects most likely reflect interactions between *APOE*, obesity and an individuals' polygenic risk for dementia.

With regards to potential mechanisms, we explored whether vascular factors (systolic and diastolic BP, BP medication) as well as inflammation-related plasma markers (CRP, IL-8, leptin/adiponectin ratio) were moderating risk effects on white matter MPF. Hypertension

is a well-established risk factor for vascular cognitive impairment, small vessel disease, and LOAD (Iulita and Girouard, 2017; Sierra, 2020). Consistent with previous findings suggesting that hypertension is associated with small vessel lesions that can result in white matter myelin damage (Fan et al., 2015), we found adverse effects of high systolic BP on white matter MPF. In addition, after the inclusion of BP covariates, there was only a trend for the three-way risk interaction, suggesting that hypertension contributed to the combined effects of risk on white matter myelin. Furthermore, while no omnibus effects of CRP, IL-8 or the leptin/adiponectin ratio were observed, including these covariates removed the interaction between *APOE*, FH and WHR. Concentrations of CRP and IL-8 in blood plasma increase in response to inflammation. Leptin and adiponectin are involved in the modulation of inflammatory responses and glucose control (Arnoldussen et al., 2014). Leptin is known to up-regulate pro-inflammatory cytokines, while adiponectin down-regulates the release and the expression of pro-inflammatory cytokines (López-Jaramillo et al., 2014). Central obesity is known to be associated with an imbalance between increased leptin and reduced adiponectin, and hence the ratio between leptin and adiponectin may be a sensitive marker of obesity‑related inflammatory states as well as of insulin resistance (Frühbeck et al., 2018) (Lopez-Jaramillo et al., 2014). *APOE-ε4* carriers have an increased risk for cardiovascular disease and metabolic syndromes (Jones and Rebeck, 2018) and *APOE* has recently been reported to attenuate the effects of inflammation (Yin et al., 2019). Together our findings suggest that the complex interactions between central obesity and genetic risk of LOAD were moderated by impaired vasculature and inflammatory processes. This conclusion is in line with previous studies that have shown that proinflammatory cytokines mediated the contributions of visceral obesity to deep white matter lesions and cognitive impairments (Lampe et al., 2019; Zhang et al., 2018).

Besides vascular and inflammatory mechanisms, it is also feasible that differences in lipid metabolism may have contributed to the effects. As myelin synthesis and maintenance are highly sensitive to cholesterol concentrations, and both *APOE-ε4* and obesity are

associated with hypercholesterolemia (Jones and Rebeck, 2018), it is possible that differences in cholesterol metabolism pathways may adversely interact with vascular and inflammatory mechanisms. Although cholesterol concentrations in the brain are largely independent of peripheral cholesterol levels, there is evidence of positive associations between white matter microstructure and serum cholesterol (Warstadt et al., 2014) and cognition (Lamar et al., 2019; Waldstein and Elias, 2001). In contrast, hypercholesterolemia in older adults or the presence of other cardiovascular risk factors is associated with lower white matter microstructure and increased risk of LOAD (Alfaro et al., 2018; Lamar et al., 2019; Shobab et al., 2005). Positive associations between white matter microstructure and allele dosage of the cholesterol gene CETP (cholesteryl ester transfer protein), which can influence the *APOE*-related risk of LOAD (Arias-Vasquez et al., 2007), were also observed for young individuals while the opposite pattern was found for older adults (Warstadt et al., 2014). Furthermore Birdsill et al. (Birdsill et al., 2017) reported greater waist circumference to be associated with larger fractional anisotropy and lower white matter diffusivities in middle-aged community-dwelling individuals, while other studies found obesity-related reductions of white matter microstructure (Kullmann et al., 2016; Kullmann et al., 2015). In combination these results suggest that the direction of obesity effects on white matter microstructure may dependent on combined effects of genetic (polygenic risk, *APOE*) and demographic (age, sex) factors that need to be taken into account in future obesity imaging studies.

In light of this evidence one may speculate that *APOE*-ε4 in combination with other polygenic risk factors potentially captured, at least in part, by family history, interacts adversely with obesity and triggers accelerated myelin damage and impaired myelin repair. Myelin decline may be particularly pronounced in obese *APOE*-ε4 carriers with a family history, due to a combination of metabolic, vascular, and inflammatory processes that cause myelin damage in the presence of inefficient cholesterol transport for myelin repair. In contrast, obese individuals without genetic risk of LOAD and other cardiovascular or

demographic risk factors, may exhibit larger white matter myelin due to hypercholesterolemia. Such complex interactions between genetic factors and vascular, inflammation and lipid pathways may potentially hold an explanation for the "obesity paradox", that refers to studies in the literature that have reported protective effects of obesity in older age with regards to brain health (Birdsill et al 2017) and dementia risk (Qizilbash et al., 2015).

Finally, a number of limitations of our research need to be considered. CARDS is a cross-sectional study that cannot answer whether the observed risk effects on MPF are predictive of accelerated development of LOAD pathology, cognitive or neuronal decline. Future prospective longitudinal studies are required to address these questions. Such studies should also include GWAS based information about individuals' polygenic risk of LOAD, and a more comprehensive investigation of inflammatory, vascular, lipid and glucose/insulin moderators to inform about potential mechanisms. It would also be worth-wile to quantify white matter hyperintensities with T_2-weighted or Fluid-Attenuated Inversion Recovery (FLAIR) MRI to assess more directly whether reductions in white matter MPF are linked to vascular events. We also propose that our findings require replication in a larger sample as the number of participants in the different risk profile subgroups was small.

It has recently been observed that head motions are more prominent in obese than normal weighted cohorts (Beyer et al., 2020). In the present study HARDI but not qMT data were corrected for motion artefacts. Therefore, the possibility that obesity-related head motion may have contributed to our results must be considered. However, a significant proportion of MR images were visually inspected for motion artefacts, extreme outlier data were removed from the statistical analyses and no significant main effects of WHR on the qMT or NODDI metrics were present. Together this makes it unlikely that a systematic obesity-related motion artefact was driving our results.

With regards to the CARDS cohort we would like to mention that eight participants had a PHQ score of ≥ 10 suggesting moderate levels of depression and two participants reported high weekly alcohol consumption of 42 and 60 units. While these participants were

not excluded from the main statistical modelling, we did check that their exclusion did not change our findings. Given the high obesity frequency in CARDS it was also surprising that so few participants self-reported a diagnosis of diabetes mellitus. It is therefore possible that some participants had Type II diabetes but were unaware of this due to a lack of a formal diagnosis. Finally, as CARDS participants ranged from 30 – 71 years in age and age is known to interact with *APOE*, family history and obesity factors, it is possible that age may also have moderated the risk effects observed here. Notably, parents of younger participants in their 40s may not have developed late-onset dementia yet, which will have resulted in an underestimation of the presence of family history of dementia in this age group. The current study therefore controlled for the effects of age in the statistical modelling of risk effects. However, future research could further evaluate the interaction between age and risk in the CARDS cohort and could collect additional information about grandparents' history of dementia.

5. References

Adluru, N., Destiche, D.J., Lu, S.Y., Doran, S.T., Birdsill, A.C., Melah, K.E., Okonkwo, O.C., Alexander, A.L., Dowling, N.M., Johnson, S.C., Sager, M.A., Bendlin, B.B., 2014. White matter microstructure in late middle-age: Effects of apolipoprotein E4 and parental family history of Alzheimer's disease. Neuroimage Clin 4, 730-742.

Alfaro, F.J., Gavrieli, A., Saade-Lemus, P., Lioutas, V.A., Upadhyay, J., Novak, V., 2018. White matter microstructure and cognitive decline in metabolic syndrome: a review of diffusion tensor imaging. Metabolism 78, 52-68.

Altmann, A., Tian, L., Henderson, V.W., Greicius, M.D., Investigators, A.s.D.N.I., 2014. Sex modifies the APOE-related risk of developing Alzheimer disease. Ann Neurol 75(4), 563-573.

Amaral, R.S.C., Park, M.T.M., Devenyi, G.A., Lynn, V., Pipitone, J., Winterburn, J., Chavez, S., Schira, M., Lobaugh, N.J., Voineskos, A.N., Pruessner, J.C., Chakravarty, M.M., Initiative, A.s.D.N., 2018. Manual segmentation of the fornix, fimbria, and alveus on high-resolution 3T MRI: Application via fully-automated mapping of the human memory circuit white and grey matter in healthy and pathological aging. Neuroimage 170, 132-150.

Arias-Vasquez, A., Isaacs, A., Aulchenko, Y.S., Hofman, A., Oostra, B.A., Breteler, M., van Duijn, C.M., 2007. The cholesteryl ester transfer protein (CETP) gene and the risk of Alzheimer's disease. Neurogenetics 8(3), 189-193.

Arnoldussen, I.A., Kiliaan, A.J., Gustafson, D.R., 2014. Obesity and dementia: adipokines interact with the brain. Eur Neuropsychopharmacol 24(12), 1982-1999.

Aschenbrenner, A.J., Balota, D.A., Gordon, B.A., Ratcliff, R., Morris, J.C., 2016. A diffusion model analysis of episodic recognition in preclinical individuals with a family history for Alzheimer's disease: The adult children study. Neuropsychology 30(2), 225-238.

Bartzokis, G., 2004. Age-related myelin breakdown: a developmental model of cognitive decline and Alzheimer's disease. Neurobiol Aging 25(1), 5-18; author reply 49-62.

Bartzokis, G., 2011. Alzheimer's disease as homeostatic responses to age-related myelin breakdown., Neurobiology of Aging. pp. 1341-1371.

Bartzokis, G., Lu, P.H., Tingus, K., Mendez, M.F., Richard, A., Peters, D.G., Oluwadara, B., Barrall, K.A., Finn, J.P., Villablanca, P., Thompson, P.M., Mintz, J., 2010. Lifespan trajectory of myelin integrity and maximum motor speed. Neurobiol Aging 31(9), 1554-1562.

Beaulieu, C., Allen, P.S., 1994. Water diffusion in the giant axon of the squid: implications for diffusion-weighted MRI of the nervous system. Magn Reson Med 32(5), 579-583.

Bendlin, B.B., Ries, M.L., Canu, E., Sodhi, A., Lazar, M., Alexander, A.L., Carlsson, C.M., Sager, M.A., Asthana, S., Johnson, S.C., 2010. White matter is altered with parental family history of Alzheimer's disease. Alzheimers Dement 6(5), 394-403.

Benjamini, Y., Hochberg, Y., 1995. Controlling the false discovery rate: a practical and powerful approach to multiple testing. . Journal of the Royal Statistical Society B 57   289-300.

Beydoun, M.A., Beydoun, H.A., Wang, Y., 2008. Obesity and central obesity as risk factors for incident dementia and its subtypes: a systematic review and meta-analysis. Obes Rev 9(3), 204-218.

Beyer, F., Prehn, K., Wüsten, K.A., Villringer, A., Ordemann, J., Flöel, A., Witte, A.V., 2020. Weight loss reduces head motion: Revisiting a major confound in neuroimaging. Hum Brain Mapp.

Birdsill, A.C., Oleson, S., Kaur, S., Pasha, E., Ireton, A., Tanaka, H., Haley, A., 2017. Abdominal obesity and white matter microstructure in midlife. Hum Brain Mapp.

Bloss, C.S., Delis, D.C., Salmon, D.P., Bondi, M.W., 2008. Decreased cognition in children with risk factors for Alzheimer's disease. Biol Psychiatry 64(10), 904-906.

Bondi, M.W., Salmon, D.P., Monsch, A.U., Galasko, D., Butters, N., Klauber, M.R., Thal, L.J., Saitoh, T., 1995. Episodic memory changes are associated with the APOE-epsilon 4 allele in nondemented older adults. Neurology 45(12), 2203-2206.

Braak, H., Del Trecidi, K., 2015. Neuroanatomy and pathology of sporadic Alzheimer's disease. Adv Anat Embryol Cell Biol 215, 1-162.

Braak, H., Del Tredici, K., 2015. The preclinical phase of the pathological process underlying sporadic Alzheimer's disease. Brain 138(Pt 10), 2814-2833.

Bradl, M., Lassmann, H., 2010. Oligodendrocytes: biology and pathology. Acta Neuropathol 119(1), 37-53.

Bubb, E.J., Metzler-Baddeley, C., Aggleton, J.P., 2018. The cingulum bundle: Anatomy, function, and dysfunction. Neurosci Biobehav Rev 92, 104-127.

Callaghan, M.F., Helms, G., Lutti, A., Mohammadi, S., Weiskopf, N., 2015. A general linear relaxometry model of R1 using imaging data. Magn Reson Med 73(3), 1309-1314.

Cattell, R.B., 1952. Factor analysis. Harper, New York.

Cercignani, M., Alexander, D.C., 2006. Optimal acquisition schemes for in vivo quantitative magnetization transfer MRI. Magn Reson Med 56(4), 803-810.

Chan, D., Gallaher, L.M., Moodley, K., Minati, L., Burgess, N., Hartley, T., 2016. The 4 Mountains Test: A Short Test of Spatial Memory with High Sensitivity for the Diagnosis of Pre-dementia Alzheimer's Disease. J Vis Exp(116).

Chen, Y., Chen, K., Zhang, J., Li, X., Shu, N., Wang, J., Zhang, Z., Reiman, E.M., 2015. Disrupted functional and structural networks in cognitively normal elderly subjects with the APOE varepsilon4 allele. Neuropsychopharmacology 40(5), 1181-1191.

Chuang, Y.F., An, Y., Bilgel, M., Wong, D.F., Troncoso, J.C., O'Brien, R.J., Breitner, J.C., Ferruci, L., Resnick, S.M., Thambisetty, M., 2016. Midlife adiposity predicts earlier onset of Alzheimer's dementia, neuropathology and presymptomatic cerebral amyloid accumulation. Mol Psychiatry 21(7), 910-915.

Chételat, G., Fouquet, M., 2013. Neuroimaging biomarkers for Alzheimer's disease in asymptomatic APOE4 carriers. Rev Neurol (Paris) 169(10), 729-736.

Coad, B., Craig, E., Louch, R., Aggleton, J., Vann, S., Metzler-Baddeley, C., 2020. Precommissural and postcommissural fornix microstructure in healthy aging and cognition., *Brain and Neuroscience Advances* 10.1177/2398212819899316.

Colgan, N., Siow, B., O'Callaghan, J.M., Harrison, I.F., Wells, J.A., Holmes, H.E., Ismail, O., Richardson, S., Alexander, D.C., Collins, E.C., Fisher, E.M., Johnson, R., Schwarz, A.J., Ahmed, Z., O'Neill, M.J., Murray, T.K., Zhang, H., Lythgoe, M.F., 2016. Application of neurite

orientation dispersion and density imaging (NODDI) to a tau pathology model of Alzheimer's disease. Neuroimage 125, 739-744.

Cox, A.J., West, N.P., Cripps, A.W., 2015. Obesity, inflammation, and the gut microbiota. Lancet Diabetes Endocrinol 3(3), 207-215.

Cramer, A.O.J., van Ravenswaaij, D., Matzke, D., Steingroever, H., Wetzels, R., Grasman, R.P.P.P., Waldrop, L.J., Wagenmakers, E.-J., 2016. Hidden multiplicity in exploratory multiway ANOVA: Prevalence and remedies. Psychonomic Bulletin Review 23, 640-647.

Daducci, A., Canales-Rodríguez, E.J., Zhang, H., Dyrby, T.B., Alexander, D.C., Thiran, J.P., 2015. Accelerated Microstructure Imaging via Convex Optimization (AMICO) from diffusion MRI data. Neuroimage 105, 32-44.

Damoiseaux, J.S., Seeley, W.W., Zhou, J., Shirer, W.R., Coppola, G., Karydas, A., Rosen, H.J., Miller, B.L., Kramer, J.H., Greicius, M.D., Initiative, A.s.D.N., 2012. Gender modulates the APOE ε4 effect in healthy older adults: convergent evidence from functional brain connectivity and spinal fluid tau levels. J Neurosci 32(24), 8254-8262.

de Chaves, E.P., Narayanaswami, V., 2008. Apolipoprotein E and cholesterol in aging and disease in the brain. Future Lipidol 3(5), 505-530.

De Santis, S., Drakesmith, M., Bells, S., Assaf, Y., Jones, D.K., 2014. Why diffusion tensor MRI does well only some of the time: variance and covariance of white matter tissue microstructure attributes in the living human brain. Neuroimage 89, 35-44.

De Strooper, B., Karran, E., 2016. The Cellular Phase of Alzheimer's Disease. Cell 164(4), 603-615.

Dell'Acqua, F., Khan, W., Gottlieb, N., Giampietro, V., Ginestet, C., Bouls, D., Newhouse, S., Dobson, R., Banaschewski, T., Barker, G.J., Bokde, A.L., Büchel, C., Conrod, P., Flor, H., Frouin, V., Garavan, H., Gowland, P., Heinz, A., Lemaítre, H., Nees, F., Paus, T., Pausova, Z., Rietschel, M., Smolka, M.N., Ströhle, A., Gallinat, J., Westman, E., Schumann, G., Lovestone, S., Simmons, A., (http://www.imagen-europe.com), I.c., 2015. Tract Based Spatial Statistic Reveals No Differences in White Matter Microstructural Organization

between Carriers and Non-Carriers of the APOE ε4 and ε2 Alleles in Young Healthy Adolescents. J Alzheimers Dis 47(4), 977-984.

Dell'acqua, F., Scifo, P., Rizzo, G., Catani, M., Simmons, A., Scotti, G., Fazio, F., 2010. A modified damped Richardson-Lucy algorithm to reduce isotropic background effects in spherical deconvolution. Neuroimage 49(2), 1446-1458.

Dick, F., Tierney, A.T., Lutti, A., Josephs, O., Sereno, M.I., Weiskopf, N., 2012. In vivo functional and myeloarchitectonic mapping of human primary auditory areas. J Neurosci 32(46), 16095-16105.

Douet, V., Chang, L., 2014. Fornix as an imaging marker for episodic memory deficits in healthy aging and in various neurological disorders. Front Aging Neurosci 6, 343.

Eng, J., Ceckler, T.L., Balaban, R.S., 1991. Quantitative 1H magnetization transfer imaging in vivo. Magn Reson Med 17(2), 304-314.

Fan, Y., Lan, L., Zheng, L., Ji, X., Lin, J., Zeng, J., Huang, R., Sun, J., 2015. Spontaneous white matter lesion in brain of stroke-prone renovascular hypertensive rats: a study from MRI, pathology and behavior. Metab Brain Dis 30(6), 1479-1486.

Fields, R.D., 2014. Neuroscience. Myelin--more than insulation. Science 344(6181), 264-266.

Fields, R.D., Araque, A., Johansen-Berg, H., Lim, S.S., Lynch, G., Nave, K.A., Nedergaard, M., Perez, R., Sejnowski, T., Wake, H., 2014. Glial Biology in Learning and Cognition. Neuroscientist 20(5), 426-431.

Fields, R.D., Dutta, D.J., 2019. Treadmilling Model for Plasticity of the Myelin Sheath. Trends Neurosci 42(7), 443-447.

Filippini, N., Ebmeier, K.P., MacIntosh, B.J., Trachtenberg, A.J., Frisoni, G.B., Wilcock, G.K., Beckmann, C.F., Smith, S.M., Matthews, P.M., Mackay, C.E., 2011. Differential effects of the APOE genotype on brain function across the lifespan. Neuroimage 54(1), 602-610.

Flechsig, P., 1920. Anatomie des menschlichen Gehirns und Rückenmarks auf myelogenetischer Grundlage. Georg Thieme, Leipzig.

Folstein, M., Folstein, S., McHugh, P., 1975. "Mini-mental state". A practical method for grading the cognitive state of patients for the clinician. . J Psychiatr Res. 12, 189–198.

Frühbeck, G., Catalán, V., Rodríguez, A., Gómez-Ambrosi, J., 2018. Adiponectin-leptin ratio: A promising index to estimate adipose tissue dysfunction. Relation with obesity-associated cardiometabolic risk. Adipocyte 7(1), 57-62.

Fu, X., Shrestha, S., Sun, M., Wu, Q., Luo, Y., Zhang, X., Yin, J., Ni, H., 2019. Microstructural White Matter Alterations in Mild Cognitive Impairment and Alzheimer's Disease : Study Based on Neurite Orientation Dispersion and Density Imaging (NODDI). Clin Neuroradiol.

Gaignard, P., Fréchou, M., Liere, P., Thérond, P., Schumacher, M., Slama, A., Guennoun, R., 2018. Sex differences in brain mitochondrial metabolism: influence of endogenous steroids and stroke. J Neuroendocrinol 30(2).

Gaignard, P., Liere, P., Thérond, P., Schumacher, M., Slama, A., Guennoun, R., 2017. Role of Sex Hormones on Brain Mitochondrial Function, with Special Reference to Aging and Neurodegenerative Diseases. Front Aging Neurosci 9, 406.

Gaignard, P., Savouroux, S., Liere, P., Pianos, A., Thérond, P., Schumacher, M., Slama, A., Guennoun, R., 2015. Effect of Sex Differences on Brain Mitochondrial Function and Its Suppression by Ovariectomy and in Aged Mice. Endocrinology 156(8), 2893-2904.

Ghebranious, N., Mukesh, B., Giampietro, P.F., Glurich, I., Mickel, S.F., Waring, S.C., McCarty, C.A., 2011. A pilot study of gene/gene and gene/environment interactions in Alzheimer disease. Clin Med Res 9(1), 17-25.

Giulietti, G., Bozzali, M., Figura, V., Spanò, B., Perri, R., Marra, C., Lacidogna, G., Giubilei, F., Caltagirone, C., Cercignani, M., 2012. Quantitative magnetization transfer provides information complementary to grey matter atrophy in Alzheimer's disease brains. Neuroimage 59(2), 1114-1122.

Gong, J.S., Kobayashi, M., Hayashi, H., Zou, K., Sawamura, N., Fujita, S.C., Yanagisawa, K., Michikawa, M., 2002. Apolipoprotein E (ApoE) isoform-dependent lipid release from

astrocytes prepared from human ApoE3 and ApoE4 knock-in mice. J Biol Chem 277(33), 29919-29926.

Gottesman, R.F., Schneider, A.L., Zhou, Y., Chen, X., Green, E., Gupta, N., Knopman, D.S., Mintz, A., Rahmim, A., Sharrett, A.R., Wagenknecht, L.E., Wong, D.F., Mosley, T.H., Jr., 2016. The ARIC-PET amyloid imaging study: Brain amyloid differences by age, race, sex, and APOE. Neurology 87(5), 473-480.

Gulland, A., 2012. Number of people with dementia will reach 65.7 million by 2030, says report. BMJ 344, e2604.

Hamilton, D., Driscoll, I., Sutherland, R., 2002. Human place learning in a virtual Morris water task: some important constraints on the flexibility of place navigation, Behavioral Brain Research. pp. 159-170.

Hampshire, A., Highfield, R.R., Parkin, B.L., Owen, A.M., 2012. Fractionating human intelligence. Neuron 76(6), 1225-1237.

Harrison, N.A., Cooper, E., Dowell, N.G., Keramida, G., Voon, V., Critchley, H.D., Cercignani, M., 2015. Quantitative Magnetization Transfer Imaging as a Biomarker for Effects of Systemic Inflammation on the Brain. Biol Psychiatry 78(1), 49-57.

Heneka, M.T., 2017. Inflammasome activation and innate immunity in Alzheimer's disease. Brain Pathol 27(2), 220-222.

Henkelman, R.M., Huang, X., Xiang, Q.S., Stanisz, G.J., Swanson, S.D., Bronskill, M.J., 1993. Quantitative interpretation of magnetization transfer. Magn Reson Med 29(6), 759-766.

Henkelman, R.M., Stanisz, G.J., Graham, S.J., 2001. Magnetization transfer in MRI: a review. NMR Biomed 14(2), 57-64.

Hersi, M., Irvine, B., Gupta, P., Gomes, J., Birkett, N., Krewski, D., 2017. Risk factors associated with the onset and progression of Alzheimer's disease: a systematic review of the evidence. Neurotoxicology.

Hu, X., Hicks, C.W., He, W., Wong, P., Macklin, W.B., Trapp, B.D., Yan, R., 2006. Bace1 modulates myelination in the central and peripheral nervous system. Nat Neurosci 9(12), 1520-1525.

Hu, X., Hou, H., Bastian, C., He, W., Qiu, S., Ge, Y., Yin, X., Kidd, G.J., Brunet, S., Trapp, B.D., Baltan, S., Yan, R., 2017. BACE1 regulates the proliferation and cellular functions of Schwann cells. Glia 65(5), 712-726.

IBM, 2011. SPSS Statistics, Version 20.0. IBM Corp., Armonk, NY.

Irfanoglu, M.O., Walker, L., Sarlls, J., Marenco, S., Pierpaoli, C., 2012. Effects of image distortions originating from susceptibility variations and concomitant fields on diffusion MRI tractography results. Neuroimage 61(1), 275-288.

Iulita, M.F., Girouard, H., 2017. Treating Hypertension to Prevent Cognitive Decline and Dementia: Re-Opening the Debate. Adv Exp Med Biol 956, 447-473.

Jack, C.R., Knopman, D.S., Jagust, W.J., Petersen, R.C., Weiner, M.W., Aisen, P.S., Shaw, L.M., Vemuri, P., Wiste, H.J., Weigand, S.D., Lesnick, T.G., Pankratz, V.S., Donohue, M.C., Trojanowski, J.Q., 2013. Tracking pathophysiological processes in Alzheimer's disease: an updated hypothetical model of dynamic biomarkers. Lancet Neurol 12(2), 207-216.

Jenkinson, M., Beckmann, C.F., Behrens, T.E., Woolrich, M.W., Smith, S.M., 2012. FSL. Neuroimage 62(2), 782-790.

Jezzard, P., Balaban, R.S., 1995. Correction for geometric distortion in echo planar images from B0 field variations. Magn Reson Med 34(1), 65-73.

Jones, D.K., Horsfield, M.A., Simmons, A., 1999. Optimal strategies for measuring diffusion in anisotropic systems by magnetic resonance imaging. Magn Reson Med 42(3), 515-525.

Jones, N.S., Rebeck, G.W., 2018. The Synergistic Effects of APOE Genotype and Obesity on Alzheimer's Disease Risk. Int J Mol Sci 20(1).

Kantarci, K., Lowe, V., Przybelski, S.A., Weigand, S.D., Senjem, M.L., Ivnik, R.J., Preboske, G.M., Roberts, R., Geda, Y.E., Boeve, B.F., Knopman, D.S., Petersen, R.C., Jack, C.R., Jr., 2012. APOE modifies the association between Abeta load and cognition in cognitively normal older adults. Neurology 78(4), 232-240.

Klein, S., Staring, M., Murphy, K., Viergever, M.A., Pluim, J.P., 2010. elastix: a toolbox for intensity-based medical image registration. IEEE Trans Med Imaging 29(1), 196-205.

Kroenke, K., Spitzer, R.L., Williams, J.B., 2001. The PHQ-9: validity of a brief depression severity measure. J Gen Intern Med 16(9), 606-613.

Kullmann, S., Callaghan, M.F., Heni, M., Weiskopf, N., Scheffler, K., Häring, H.U., Fritsche, A., Veit, R., Preissl, H., 2016. Specific white matter tissue microstructure changes associated with obesity. Neuroimage 125, 36-44.

Kullmann, S., Schweizer, F., Veit, R., Fritsche, A., Preissl, H., 2015. Compromised white matter integrity in obesity. Obes Rev 16(4), 273-281.

Kunkle, B.W., Grenier-Boley, B., Sims, R., Bis, J.C., Damotte, V., Naj, A.C., Boland, A., Vronskaya, M., van der Lee, S.J., Amlie-Wolf, A., Bellenguez, C., Frizatti, A., Chouraki, V., Martin, E.R., Sleegers, K., Badarinarayan, N., Jakobsdottir, J., Hamilton-Nelson, K.L., Moreno-Grau, S., Olaso, R., Raybould, R., Chen, Y., Kuzma, A.B., Hiltunen, M., Morgan, T., Ahmad, S., Vardarajan, B.N., Epelbaum, J., Hoffmann, P., Boada, M., Beecham, G.W., Garnier, J.G., Harold, D., Fitzpatrick, A.L., Valladares, O., Moutet, M.L., Gerrish, A., Smith, A.V., Qu, L., Bacq, D., Denning, N., Jian, X., Zhao, Y., Del Zompo, M., Fox, N.C., Choi, S.H., Mateo, I., Hughes, J.T., Adams, H.H., Malamon, J., Sanchez-Garcia, F., Patel, Y., Brody, J.A., Dombroski, B.A., Naranjo, M.C.D., Daniilidou, M., Eiriksdottir, G., Mukherjee, S., Wallon, D., Uphill, J., Aspelund, T., Cantwell, L.B., Garzia, F., Galimberti, D., Hofer, E., Butkiewicz, M., Fin, B., Scarpini, E., Sarnowski, C., Bush, W.S., Meslage, S., Kornhuber, J., White, C.C., Song, Y., Barber, R.C., Engelborghs, S., Sordon, S., Voijnovic, D., Adams, P.M., Vandenberghe, R., Mayhaus, M., Cupples, L.A., Albert, M.S., De Deyn, P.P., Gu, W., Himali, J.J., Beekly, D., Squassina, A., Hartmann, A.M., Orellana, A., Blacker, D., Rodriguez-Rodriguez, E., Lovestone, S., Garcia, M.E., Doody, R.S., Munoz-Fernadez, C., Sussams, R., Lin, H., Fairchild, T.J., Benito, Y.A., Holmes, C., Karamujic-Comic, H., Frosch, M.P., Thonberg, H., Maier, W., Roshchupkin, G., Ghetti, B., Giedraitis, V., Kawalia, A., Li, S., Huebinger, R.M., Kilander, L., Moebus, S., Hernandez, I., Kamboh, M.I., Brundin, R., Turton, J., Yang, Q., Katz, M.J., Concari, L., Lord, J., Beiser, A.S., Keene, C.D., Helisalmi, S.,

Kloszewska, I., Kukull, W.A., Koivisto, A.M., Lynch, A., Tarraga, L., Larson, E.B., Haapasalo, A., Lawlor, B., Mosley, T.H., Lipton, R.B., Solfrizzi, V., Gill, M., Longstreth, W.T., Jr., Montine, T.J., Frisardi, V., Diez-Fairen, M., Rivadeneira, F., Petersen, R.C., Deramecourt, V., Alvarez, I., Salani, F., Ciaramella, A., Boerwinkle, E., Reiman, E.M., Fievet, N., Rotter, J.I., Reisch, J.S., Hanon, O., Cupidi, C., Andre Uitterlinden, A.G., Royall, D.R., Dufouil, C., Maletta, R.G., de Rojas, I., Sano, M., Brice, A., Cecchetti, R., George-Hyslop, P.S., Ritchie, K., Tsolaki, M., Tsuang, D.W., Dubois, B., Craig, D., Wu, C.K., Soininen, H., Avramidou, D., Albin, R.L., Fratiglioni, L., Germanou, A., Apostolova, L.G., Keller, L., Koutroumani, M., Arnold, S.E., Panza, F., Gkatzima, O., Asthana, S., Hannequin, D., Whitehead, P., Atwood, C.S., Caffarra, P., Hampel, H., Quintela, I., Carracedo, A., Lannfelt, L., Rubinsztein, D.C., Barnes, L.L., Pasquier, F., Frolich, L., Barral, S., McGuinness, B., Beach, T.G., Johnston, J.A., Becker, J.T., Passmore, P., Bigio, E.H., Schott, J.M., Bird, T.D., Warren, J.D., Boeve, B.F., Lupton, M.K., Bowen, J.D., Proitsi, P., Boxer, A., Powell, J.F., Burke, J.R., Kauwe, J.S.K., Burns, J.M., Mancuso, M., Buxbaum, J.D., Bonuccelli, U., Cairns, N.J., McQuillin, A., Cao, C., Livingston, G., Carlson, C.S., Bass, N.J., Carlsson, C.M., Hardy, J., Carney, R.M., Bras, J., Carrasquillo, M.M., Guerreiro, R., Allen, M., Chui, H.C., Fisher, E., Masullo, C., Crocco, E.A., DeCarli, C., Bisceglio, G., Dick, M., Ma, L., Duara, R., Graff-Radford, N.R., Evans, D.A., Hodges, A., Faber, K.M., Scherer, M., Fallon, K.B., Riemenschneider, M., Fardo, D.W., Heun, R., Farlow, M.R., Kolsch, H., Ferris, S., Leber, M., Foroud, T.M., Heuser, I., Galasko, D.R., Giegling, I., Gearing, M., Hull, M., Geschwind, D.H., Gilbert, J.R., Morris, J., Green, R.C., Mayo, K., Growdon, J.H., Feulner, T., Hamilton, R.L., Harrell, L.E., Drichel, D., Honig, L.S., Cushion, T.D., Huentelman, M.J., Hollingworth, P., Hulette, C.M., Hyman, B.T., Marshall, R., Jarvik, G.P., Meggy, A., Abner, E., Menzies, G.E., Jin, L.W., Leonenko, G., Real, L.M., Jun, G.R., Baldwin, C.T., Grozeva, D., Karydas, A., Russo, G., Kaye, J.A., Kim, R., Jessen, F., Kowall, N.W., Vellas, B., Kramer, J.H., Vardy, E., LaFerla, F.M., Jockel, K.H., Lah, J.J., Dichgans, M., Leverenz, J.B., Mann, D., Levey, A.I., Pickering-Brown, S., Lieberman, A.P., Klopp, N., Lunetta, K.L., Wichmann, H.E., Lyketsos, C.G., Morgan, K., Marson, D.C., Brown, K., Martiniuk, F., Medway, C., Mash, D.C., Nothen, M.M., Masliah, E.,

Hooper, N.M., McCormick, W.C., Daniele, A., McCurry, S.M., Bayer, A., McDavid, A.N., Gallacher, J., McKee, A.C., van den Bussche, H., Mesulam, M., Brayne, C., Miller, B.L., Riedel-Heller, S., Miller, C.A., Miller, J.W., Al-Chalabi, A., Morris, J.C., Shaw, C.E., Myers, A.J., Wiltfang, J., O'Bryant, S., Olichney, J.M., Alvarez, V., Parisi, J.E., Singleton, A.B., Paulson, H.L., Collinge, J., Perry, W.R., Mead, S., Peskind, E., Cribbs, D.H., Rossor, M., Pierce, A., Ryan, N.S., Poon, W.W., Nacmias, B., Potter, H., Sorbi, S., Quinn, J.F., Sacchinelli, E., Raj, A., Spalletta, G., Raskind, M., Caltagirone, C., Bossu, P., Orfei, M.D., Reisberg, B., Clarke, R., Reitz, C., Smith, A.D., Ringman, J.M., Warden, D., Roberson, E.D., Wilcock, G., Rogaeva, E., Bruni, A.C., Rosen, H.J., Gallo, M., Rosenberg, R.N., Ben-Shlomo, Y., Sager, M.A., Mecocci, P., Saykin, A.J., Pastor, P., Cuccaro, M.L., Vance, J.M., Schneider, J.A., Schneider, L.S., Slifer, S., Seeley, W.W., Smith, A.G., Sonnen, J.A., Spina, S., Stern, R.A., Swerdlow, R.H., Tang, M., Tanzi, R.E., Trojanowski, J.Q., Troncoso, J.C., Van Deerlin, V.M., Van Eldik, L.J., Vinters, H.V., Vonsattel, J.P., Weintraub, S., Welsh-Bohmer, K.A., Wilhelmsen, K.C., Williamson, J., Wingo, T.S., Woltjer, R.L., Wright, C.B., Yu, C.E., Yu, L., Saba, Y., Pilotto, A., Bullido, M.J., Peters, O., Crane, P.K., Bennett, D., Bosco, P., Coto, E., Boccardi, V., De Jager, P.L., Lleo, A., Warner, N., Lopez, O.L., Ingelsson, M., Deloukas, P., Cruchaga, C., Graff, C., Gwilliam, R., Fornage, M., Goate, A.M., Sanchez-Juan, P., Kehoe, P.G., Amin, N., Ertekin-Taner, N., Berr, C., Debette, S., Love, S., Launer, L.J., Younkin, S.G., Dartigues, J.F., Corcoran, C., Ikram, M.A., Dickson, D.W., Nicolas, G., Campion, D., Tschanz, J., Schmidt, H., Hakonarson, H., Clarimon, J., Munger, R., Schmidt, R., Farrer, L.A., Van Broeckhoven, C., M, C.O.D., DeStefano, A.L., Jones, L., Haines, J.L., Deleuze, J.F., Owen, M.J., Gudnason, V., Mayeux, R., Escott-Price, V., Psaty, B.M., Ramirez, A., Wang, L.S., Ruiz, A., van Duijn, C.M., Holmans, P.A., Seshadri, S., Williams, J., Amouyel, P., Schellenberg, G.D., Lambert, J.C., Pericak-Vance, M.A., Alzheimer Disease Genetics, C., European Alzheimer's Disease, I., Cohorts for, H., Aging Research in Genomic Epidemiology, C., Genetic, Environmental Risk in Ad/Defining Genetic, P., Environmental Risk for Alzheimer's Disease, C., 2019. Genetic meta-analysis of diagnosed Alzheimer's

disease identifies new risk loci and implicates Abeta, tau, immunity and lipid processing. Nat Genet 51(3), 414-430.

Kunz, L., Schröder, T.N., Lee, H., Montag, C., Lachmann, B., Sariyska, R., Reuter, M., Stirnberg, R., Stöcker, T., Messing-Floeter, P.C., Fell, J., Doeller, C.F., Axmacher, N., 2015. Reduced grid-cell-like representations in adults at genetic risk for Alzheimer's disease. Science 350(6259), 430-433.

Lamar, M., Durazo-Arvizu, R.A., Rodriguez, C.J., Kaplan, R.C., Perera, M.J., Cai, J., Espinoza Giacinto, R.A., González, H.M., Daviglus, M.L., 2019. Associations of Lipid Levels and Cognition: Findings from the Hispanic Community Health Study/Study of Latinos. J Int Neuropsychol Soc, 1-12.

Lampe, L., Zhang, R., Beyer, F., Huhn, S., Kharabian Masouleh, S., Preusser, S., Bazin, P.L., Schroeter, M.L., Villringer, A., Witte, A.V., 2019. Visceral obesity relates to deep white matter hyperintensities via inflammation. Ann Neurol 85(2), 194-203.

Lancaster, M.A., Seidenberg, M., Smith, J.C., Nielson, K.A., Woodard, J.L., Durgerian, S., Rao, S.M., 2016. Diffusion Tensor Imaging Predictors of Episodic Memory Decline in Healthy Elders at Genetic Risk for Alzheimer's Disease. J Int Neuropsychol Soc 22(10), 1005-1015.

Leemans A, Jeurissen B, Sijbers J, DK., J., 2009. ExploreDTI: a graphical toolbox for processing, analyzing, and visualizing diffusion MR data., 17th Annual Meeting of Intl Soc Mag Reson Med. Hawaii, USA., p. 3537.

Leemans, A., Jones, D.K., 2009. The B-matrix must be rotated when correcting for subject motion in DTI data. Magn Reson Med 61(6), 1336-1349.

Levesque, I.R., Giacomini, P.S., Narayanan, S., Ribeiro, L.T., Sled, J.G., Arnold, D.L., Pike, G.B., 2010. Quantitative magnetization transfer and myelin water imaging of the evolution of acute multiple sclerosis lesions. Magn Reson Med 63(3), 633-640.

Lim, Y.Y., Williamson, R., Laws, S.M., Villemagne, V.L., Bourgeat, P., Fowler, C., Rainey-Smith, S., Salvado, O., Martins, R.N., Rowe, C.C., Masters, C.L., Maruff, P., Group, A.R.,

2017. Effect of APOE Genotype on Amyloid Deposition, Brain Volume, and Memory in Cognitively Normal Older Individuals. J Alzheimers Dis 58(4), 1293-1302.

Loprinzi, P.D., Frith, E., 2018. Obesity and episodic memory function. J Physiol Sci 68(4), 321-331.

Luck, T., Then, F.S., Luppa, M., Schroeter, M.L., Arelin, K., Burkhardt, R., Thiery, J., Loffler, M., Villringer, A., Riedel-Heller, S.G., 2015. Association of the apolipoprotein E genotype with memory performance and executive functioning in cognitively intact elderly. Neuropsychology 29(3), 382-387.

López-Jaramillo, P., Gómez-Arbeláez, D., López-López, J., López-López, C., Martínez-Ortega, J., Gómez-Rodríguez, A., Triana-Cubillos, S., 2014. The role of leptin/adiponectin ratio in metabolic syndrome and diabetes. Horm Mol Biol Clin Investig 18(1), 37-45.

Maghsudi, H., Schütze, M., Maudsley, A.A., Dadak, M., Lanfermann, H., Ding, X.Q., 2019. Age-related Brain Metabolic Changes up to Seventh Decade in Healthy Humans : Whole-brain Magnetic Resonance Spectroscopic Imaging Study. Clin Neuroradiol.

Mahoney-Sanchez, L., Belaidi, A.A., Bush, A.I., Ayton, S., 2016. The Complex Role of Apolipoprotein E in Alzheimer's Disease: an Overview and Update. J Mol Neurosci 60(3), 325-335.

Marioni, R.E., Harris, S.E., Zhang, Q., McRae, A.F., Hagenaars, S.P., Hill, W.D., Davies, G., Ritchie, C.W., Gale, C.R., Starr, J.M., Goate, A.M., Porteous, D.J., Yang, J., Evans, K.L., Deary, I.J., Wray, N.R., Visscher, P.M., 2018. GWAS on family history of Alzheimer's disease. Transl Psychiatry 8(1), 99.

Mattson, M.P., Arumugam, T.V., 2018. Hallmarks of Brain Aging: Adaptive and Pathological Modification by Metabolic States. Cell Metab 27(6), 1176-1199.

Metzler-Baddeley, C., Baddeley, R.J., Jones, D.K., Aggleton, J.P., O'Sullivan, M.J., 2013. Individual differences in fornix microstructure and body mass index. PLoS One 8(3), e59849.

Metzler-Baddeley, C., Hunt, S., Jones, D.K., Leemans, A., Aggleton, J.P., O'Sullivan, M.J., 2012a. Temporal association tracts and the breakdown of episodic memory in mild cognitive impairment. Neurology 79(23), 2233-2240.

Metzler-Baddeley, C., Jones, D.K., Belaroussi, B., Aggleton, J.P., O'Sullivan, M.J., 2011. Frontotemporal connections in episodic memory and aging: a diffusion MRI tractography study. J Neurosci 31(37), 13236-13245.

Metzler-Baddeley, C., Jones, D.K., Steventon, J., Westacott, L., Aggleton, J.P., O'Sullivan, M.J., 2012b. Cingulum Microstructure Predicts Cognitive Control in Older Age and Mild Cognitive Impairment. Journal of Neuroscience 32(49), 17612-17619.

Metzler-Baddeley, C., Mole, J., Leonaviciute, E., Sims, R., Kelso-Mitchell, A., Gidney, F., Fasano, F., Evans, J., Kidd, E., Ertefai, B., Jones, D., Baddeley, R., 2019a. Sex-specific effects of central adiposity and inflammatory markers on limbic microstructure., NeuroImage. pp. 793-803.

Metzler-Baddeley, C., Mole, J., Sims, R., Fasano, F., Evans, J., Jones, D., Aggleton, J., Baddeley, R., 2019b. Fornix white matter glia damage causes hippocampal gray matter damage during age-dependent limbic decline, Scientific Reports. Nature Publishing Group, p. 1060.

Metzler-Baddeley, C., Mole, J., Sims, R., Fasano, F., Evans, J., Jones, D., Aggleton, J., Baddeley, R., 2019c. Fornix white matter glia damage causes hippocampal gray matter damage during age-dependent limbic decline, Scientific Reports. Nature Publishing Group pp. 1060-1074

Nasrabady, S.E., Rizvi, B., Goldman, J.E., Brickman, A.M., 2018. White matter changes in Alzheimer's disease: a focus on myelin and oligodendrocytes. Acta Neuropathol Commun 6(1), 22.

Nave, K.A., Salzer, J.L., 2006. Axonal regulation of myelination by neuregulin 1. Curr Opin Neurobiol 16(5), 492-500.

Nelson, H.E., 1991. The National Adult Reading Test-Revised (NART-R): Test manual. National Foundation for Educational Research-Nelson., Windsor, UK.

O'Donoghue, M.C., Murphy, S.E., Zamboni, G., Nobre, A.C., Mackay, C.E., 2018a. APOE genotype and cognition in healthy individuals at risk of Alzheimer's disease: A review. Cortex 104, 103-123.

O'Donoghue, M.C., Murphy, S.E., Zamboni, G., Nobre, A.C., Mackay, C.E., 2018b. APOE genotype and cognition in healthy individuals at risk of Alzheimer's disease: A review. Cortex 104, 103-123.

Organisation, W.H., 2008. Waist Circumference and Waist-Hip-Ratio: Report of a WHO expert consultation.

Osborne, J., Costello, A., Kellow, J., 2008. Best practices in exploratory factor analysis, in: Osborne, J. (Ed.) Best practices in quantitative methods. Sage Publications.

Ossenkoppele, R., Schonhaut, D.R., Schöll, M., Lockhart, S.N., Ayakta, N., Baker, S.L., O'Neil, J.P., Janabi, M., Lazaris, A., Cantwell, A., Vogel, J., Santos, M., Miller, Z.A., Bettcher, B.M., Vossel, K.A., Kramer, J.H., Gorno-Tempini, M.L., Miller, B.L., Jagust, W.J., Rabinovici, G.D., 2016. Tau PET patterns mirror clinical and neuroanatomical variability in Alzheimer's disease. Brain 139(Pt 5), 1551-1567.

Ou, X., Sun, S.W., Liang, H.F., Song, S.K., Gochberg, D.F., 2009a. Quantitative magnetization transfer measured pool-size ratio reflects optic nerve myelin content in ex vivo mice. Magn Reson Med 61(2), 364-371.

Ou, X., Sun, S.W., Liang, H.F., Song, S.K., Gochberg, D.F., 2009b. The MT pool size ratio and the DTI radial diffusivity may reflect the myelination in shiverer and control mice. NMR Biomed 22(5), 480-487.

Owen, A.M., Hampshire, A., Grahn, J.A., Stenton, R., Dajani, S., Burns, A.S., Howard, R.J., Ballard, C.G., 2010. Putting brain training to the test. Nature 465(7299), 775-778.

Pajevic, S., Pierpaoli, C., 1999. Color schemes to represent the orientation of anisotropic tissues from diffusion tensor data: application to white matter fiber tract mapping in the human brain. Magn Reson Med 42(3), 526-540.

Parker, G., 2014. Robust processing of diffusion weighted image data. Unpublished PhD thesis, Cardiff University.

Parker, G., Rosin, P., Marshall, D., 2012. Automated segmentation of diffusion weigthed MRI tractography. Presented a the AVA, AVA/BMVA Meeting on Biological and Computer Vision Cambridge, UK.

Payami, H., Grimslid, H., Oken, B., Camicioli, R., Sexton, G., Dame, A., Howieson, D., Kaye, J., 1997. A prospective study of cognitive health in the elderly (Oregon Brain Aging Study): effects of family history and apolipoprotein E genotype. Am J Hum Genet 60(4), 948-956.

Pedditizi, E., Peters, R., Beckett, N., 2016. The risk of overweight/obesity in mid-life and late life for the development of dementia: a systematic review and meta-analysis of longitudinal studies. Age Ageing 45(1), 14-21.

Peters, A., Sethares, C., Moss, M.B., 2010. How the primate fornix is affected by age. J Comp Neurol 518(19), 3962-3980.

Pierpaoli, C., Basser, P.J., 1996. Toward a quantitative assessment of diffusion anisotropy. Magn Reson Med 36(6), 893-906.

Qizilbash, N., Gregson, J., Johnson, M., Pearce, N., Douglas, I., Wing, K., Evans, S., Pocock, S., 2015. BMI and risk of dementia in two million people over two decades: A retrospective cohort study. Lancet Diabetes Endocrinol 3, 431-436.

Ramani, A., Dalton, C., Miller, D.H., Tofts, P.S., Barker, G.J., 2002. Precise estimate of fundamental in-vivo MT parameters in human brain in clinically feasible times. Magn Reson Imaging 20(10), 721-731.

Raz, N., 2001. Ageing and the brain. Encyclopedia of Life Sciences, 1-6.

Reiman, E.M., Chen, K., Alexander, G.E., Caselli, R.J., Bandy, D., Osborne, D., Saunders, A.M., Hardy, J., 2004. Functional brain abnormalities in young adults at genetic risk for late-onset Alzheimer's dementia. Proc Natl Acad Sci U S A 101(1), 284-289.

Rey, A., 1941. L'examen psychologique dans les cas d'encephalopathie traumatique., Archives de Psychologie. pp. 215-285.

Salthouse, T.A., 1976. Speed and age: multiple rates of age decline. Exp Aging Res 2(4), 349-359.

Samsonov, A., Alexander, A.L., Mossahebi, P., Wu, Y.C., Duncan, I.D., Field, A.S., 2012. Quantitative MR imaging of two-pool magnetization transfer model parameters in myelin mutant shaking pup. Neuroimage 62(3), 1390-1398.

Sarlus, H., Heneka, M.T., 2017. Microglia in Alzheimer's disease. J Clin Invest 127(9), 3240-3249.

Schmidt, M., 1996. Rey Auditory and Verbal Learning Test. A handbook. Western Psychological Association, Los Angeles.

Schmierer, K., Tozer, D.J., Scaravilli, F., Altmann, D.R., Barker, G.J., Tofts, P.S., Miller, D.H., 2007. Quantitative magnetization transfer imaging in postmortem multiple sclerosis brain. J Magn Reson Imaging 26(1), 41-51.

Sereno, M.I., Lutti, A., Weiskopf, N., Dick, F., 2013. Mapping the human cortical surface by combining quantitative T(1) with retinotopy. Cereb Cortex 23(9), 2261-2268.

Shobab, L.A., Hsiung, G.Y., Feldman, H.H., 2005. Cholesterol in Alzheimer's disease. Lancet Neurol 4(12), 841-852.

Sierra, C., 2020. Hypertension and the Risk of Dementia. Front Cardiovasc Med 7, 5.

Slattery, C.F., Zhang, J., Paterson, R.W., Foulkes, A.J.M., Carton, A., Macpherson, K., Mancini, L., Thomas, D.L., Modat, M., Toussaint, N., Cash, D.M., Thornton, J.S., Henley, S.M.D., Crutch, S.J., Alexander, D.C., Ourselin, S., Fox, N.C., Zhang, H., Schott, J.M., 2017. ApoE influences regional white-matter axonal density loss in Alzheimer's disease. Neurobiol Aging 57, 8-17.

Sled, J.G., 2018. Modelling and interpretation of magnetization transfer imaging in the brain. Neuroimage 182, 128-135.

Sochocka, M., Donskow-Łysoniewska, K., Diniz, B.S., Kurpas, D., Brzozowska, E., Leszek, J., 2018. The Gut Microbiome Alterations and Inflammation-Driven Pathogenesis of Alzheimer's Disease-a Critical Review. Mol Neurobiol.

Stoub, T.R., Detoledo-Morrell, L., Dickerson, B.C., 2014. Parahippocampal white matter volume predicts Alzheimer's disease risk in cognitively normal old adults. Neurobiol Aging 35(8), 1855-1861.

Tang, X., Cai, F., Ding, D.X., Zhang, L.L., Cai, X.Y., Fang, Q., 2018. Magnetic resonance imaging relaxation time in Alzheimer's disease. Brain Res Bull 140, 176-189.

Tejera, D., Heneka, M.T., 2016. Microglia in Alzheimer's disease: the good, the bad and the ugly. Curr Alzheimer Res 13(4), 370-380.

Toledo, J.B., Habes, M., Sotiras, A., Bjerke, M., Fan, Y., Weiner, M.W., Shaw, L.M., Davatzikos, C., Trojanowski, J.Q., Alzheimer's Disease Neuroimaging, I., 2019. APOE Effect on Amyloid-beta PET Spatial Distribution, Deposition Rate, and Cut-Points. J Alzheimers Dis 69(3), 783-793.

Tuch, D.S., Reese, T.G., Wiegell, M.R., Makris, N., Belliveau, J.W., Wedeen, V.J., 2002. High angular resolution diffusion imaging reveals intravoxel white matter fiber heterogeneity. Magn Reson Med 48(4), 577-582.

Turner, R., 2019. Myelin and Modeling: Bootstrapping Cortical Microcircuits. Front Neural Circuits 13, 34.

Vassar, R., 2004. BACE1: the beta-secretase enzyme in Alzheimer's disease. J Mol Neurosci 23(1-2), 105-114.

Vogt, N.M., Hunt, J.F., Adluru, N., Dean, D.C., Johnson, S.C., Asthana, S., Yu, J.J., Alexander, A.L., Bendlin, B.B., 2019. Cortical Microstructural Alterations in Mild Cognitive Impairment and Alzheimer's Disease Dementia. Cereb Cortex.

Waldstein, S., Elias, M., 2001. Neuropsychology of cardiovascular disease. Lawrence Erlbaum Associates.

Warstadt, N.M., Dennis, E.L., Jahanshad, N., Kohannim, O., Nir, T.M., McMahon, K.L., de Zubicaray, G.I., Montgomery, G.W., Henders, A.K., Martin, N.G., Whitfield, J.B., Jack, C.R., Jr., Bernstein, M.A., Weiner, M.W., Toga, A.W., Wright, M.J., Thompson, P.M., Alzheimer's Disease Neuroimaging, I., 2014. Serum cholesterol and variant in cholesterol-related gene CETP predict white matter microstructure. Neurobiol Aging 35(11), 2504-2513.

Yi, D., Lee, Y., Byun, M.S., Lee, J.H., Ko, K., Sohn, B.K., Choe, Y.M., Choi, H.J., Baek, H., Sohn, C.H., Kim, Y.K., Lee, D.Y., group, K.r., 2018. Synergistic interaction between APOE

and family history of Alzheimer's disease on cerebral amyloid deposition and glucose metabolism. Alzheimers Res Ther 10(1), 84.

Yin, C., Ackermann, S., Ma, Z., Mohanta, S.K., Zhang, C., Li, Y., Nietzsche, S., Westermann, M., Peng, L., Hu, D., Bontha, S.V., Srikakulapu, P., Beer, M., Megens, R.T.A., Steffens, S., Hildner, M., Halder, L.D., Eckstein, H.H., Pelisek, J., Herms, J., Roeber, S., Arzberger, T., Borodovsky, A., Habenicht, L., Binder, C.J., Weber, C., Zipfel, P.F., Skerka, C., Habenicht, A.J.R., 2019. ApoE attenuates unresolvable inflammation by complex formation with activated C1q. Nat Med 25(3), 496-506.

Zade, D., Beiser, A., McGlinchey, R., Au, R., Seshadri, S., Palumbo, C., Wolf, P.A., DeCarli, C., Milberg, W., 2013. Apolipoprotein epsilon 4 allele modifies waist-to-hip ratio effects on cognition and brain structure. J Stroke Cerebrovasc Dis 22(2), 119-125.

Zhang, H., Schneider, T., Wheeler-Kingshott, C.A., Alexander, D.C., 2012. NODDI: practical in vivo neurite orientation dispersion and density imaging of the human brain. Neuroimage 61(4), 1000-1016.

Zhang, R., Beyer, F., Lampe, L., Luck, T., Riedel-Heller, S.G., Loeffler, M., Schroeter, M.L., Stumvoll, M., Villringer, A., Witte, A.V., 2018. White matter microstructural variability mediates the relation between obesity and cognition in healthy adults. Neuroimage 172, 239-249.

Mean (SD) (range)	Participants (n = 166)
Age (in years)	55.8 (8.2) (38 - 71)
Females	56%
Years of education	16.5 (3.3) (9.5 - 26)
NART-IQ	116.7 (6.7) (96 - 128)
MMSE	29.1 (1.0) (26 - 30)
PHQ-9	2.6 (2.9) (0 - 13)
FH+	35.1%
APOE4+	36.3% (4.2% ε4/ε4)
Abdominal obesity*	61.3%
Systolic hypertension (≥ 140 mm Hg)	28%
Systolic blood pressure (mm Hg)	131.9 (18.7) (68.3 – 196)
Diastolic blood pressure (mm Hg)	83.3 (9.4) (59 – 119)
Hypertension medication	11.5%
Smokers	5.4%
Diabetes	1.8%
Statins	7.2%
Alcohol units per week	7.4 (9.3) (0 - 60)
C-Reactive Protein (lg ng/ml)	3.1 (0.47) (1.9 - 4.3)
Interleukin 8 (lg pg/ml)	0.71 (0.15) (0.35 – 1.24)
Leptin (lg pg/ml)	4.1 (0.47) (2.7 - 4.9)
Adiponectin (lg ng/ml)	4.1 (0.26) (3.3 - 4.8)

Table 1 Summary of demographic, genetic, and lifestyle risk information of

participants.*Based on waist to hip ratio ≥ 0.9 for males and ≥ 0.85 for females

(Organisation, 2008). Abbreviations: *APOE*, Apolipoprotein-E; FH, Family History of

dementia; MMSE = Mini Mental State Exam (Folstein et al., 1975); NART = National Adult

Reading Test(Nelson, 1991); PHQ-9 = Patient Health Questionnaire (Kroenke et al., 2001).

Effect	ROI	Index	$F_{(1,107)}$-value	p_{BHadj}	r	p_{BHadj}
Age	Whole brain WM	MPF	25.4	< 0.001	-0.37	< 0.001
		ISOSF	12.0	0.008	0.30	< 0.001
		R_1	12.8	0.009	-0.30	< 0.001
		k_f	13.3	< 0.001	-0.29	< 0.001
	Fornix	MPF	29.5	< 0.001	-0.42	< 0.001
		ISOSF	18.5	< 0.001	0.32	< 0.001
		R_1	26.5	< 0.001	-0.41	< 0.001
		k_f	27.4	< 0.001	-0.41	< 0.001
	L UF	MPF	8.1	0.025	-0.21	0.008
		k_f	9.9	0.013	-0.25	0.002
	R UF	R_1	15.0	< 0.001	-0.31	< 0.001
		MPF	8.3	0.025	-0.21	0.008
		k_f	11.1	0.008	-0.24	0.003
	L CST	k_f	8.8	0.02	-0.26	0.001
	R CST	k_f	16.3	< 0.001	-0.36	< 0.001
					t-value	
Sex	Whole brain WM	k_f	18.7	< 0.001	3.46	0.004
		ISOSF	11.1	0.008	2.92	0.008
	Fornix	ISOSF	28.8	< 0.001	6.6	< 0.001
		MPF	8.7	0.02	-3.0	0.008
	L PHC	k_f	9.9	0.01		
	R PHC	k_f	13.2	< 0.001		
	L UF	k_f	9.9	0.01	ns	
	R CST	R_1	9.5	0.02		
FH x *APOE* x WHR	Whole brain WM	MPF	18.3	< 0.001	ns	
	R PHC	MPF	14.0	< 0.001	3.63[+] -3.5[++]	0.012 0.012
		ICSF	11.7	0.007	3.0[+]	0.03
	L CST	MPF	11.9	0.007		
	R CST	MPF	16.5	< 0.001		
	L UF	MPF	13.0	< 0.001	ns	
	R UF	MPF	11.4	0.007		

Table 2 Post-hoc effects on white matter microstructure. [+]Contrast: centrally obese (n = 8) relative to normal weighted (n = 10) *APOE*-ε4 carriers (*APOE*-ε2/ε4, *APOE*-ε3/ε4, *APOE*-ε4/ε4) with a family history of dementia. [++]Contrast: centrally obese (n = 13) relative to normal weighted (n = 28) *APOE*-ε4 non-carriers (*APOE*-ε2/ε2, *APOE*-ε2/ε3, *APOE*-ε3/ε3) with a family history. Abbreviations: *APOE*, Apoliopoprotein E; CST, corticospinal tract; FH, family history of dementia; ICSF, intracellular signal fraction; ISOSF, isotropic signal fraction;

k_f, forward exchange rate; MPF, macromolecular proton fraction; ODI, orientation density index; p_{BHadj}, Benjamini-Hochberg adjusted p-value; PHC, parahippocampal cingulum; R_1, longitudinal relaxation rate; ROI, region of interest; UF, uncinate fasciculus; WM, white matter.
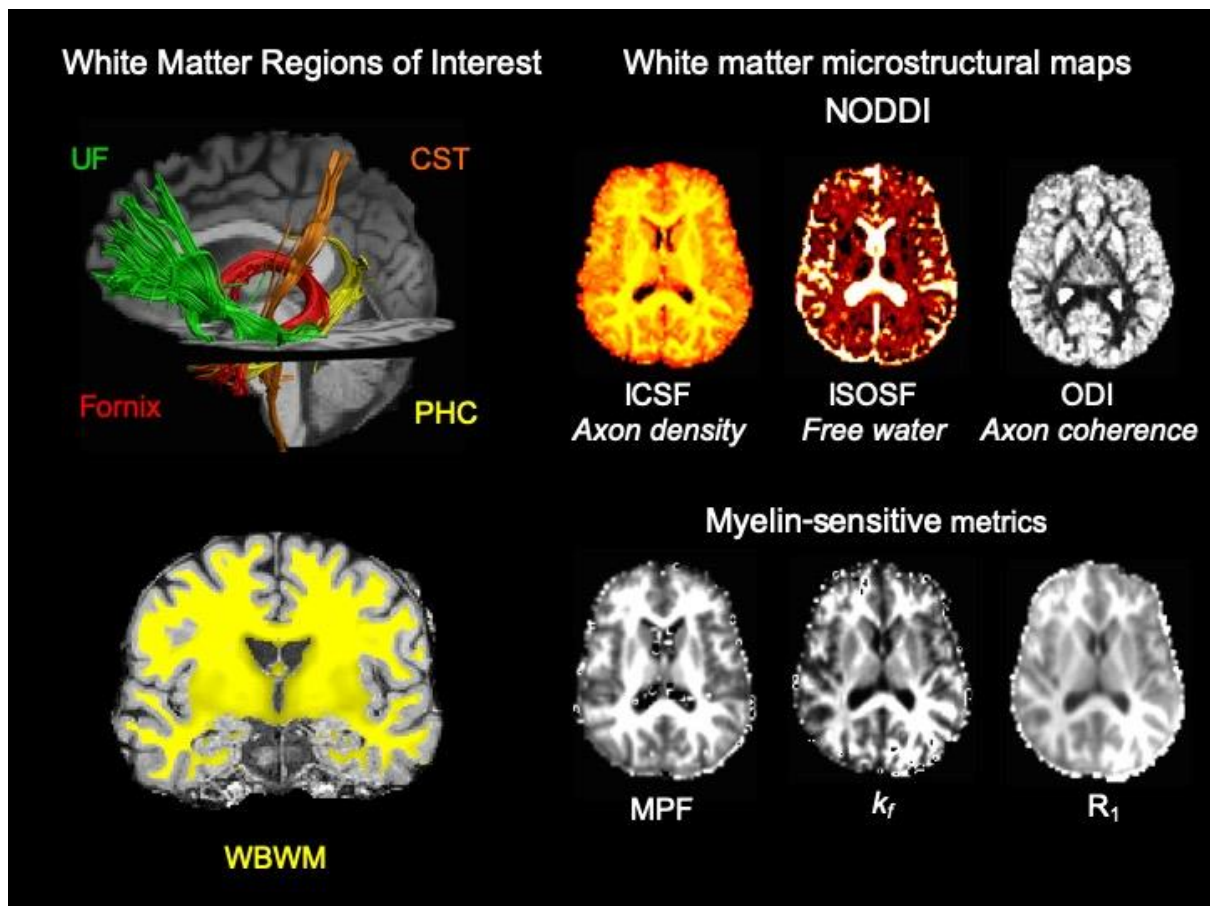
Figure 1 displays the white matter pathways and whole brain white matter region of interest as well as the microstructural maps for one representative participant. Abbreviations: CST, corticospinal tract; ICSF, intracellular signal fraction; ISOSF, isotropic signal fraction; k_f, forward exchange rate; MPF, macromolecular proton fraction; NODDI, neurite orientation dispersion and density imaging; ODI, orientation density index; PHC, parahippocampal cingulum; UF, uncinate fasciculus; R_1, longitudinal relaxation rate; WBWM, whole brain white matter.
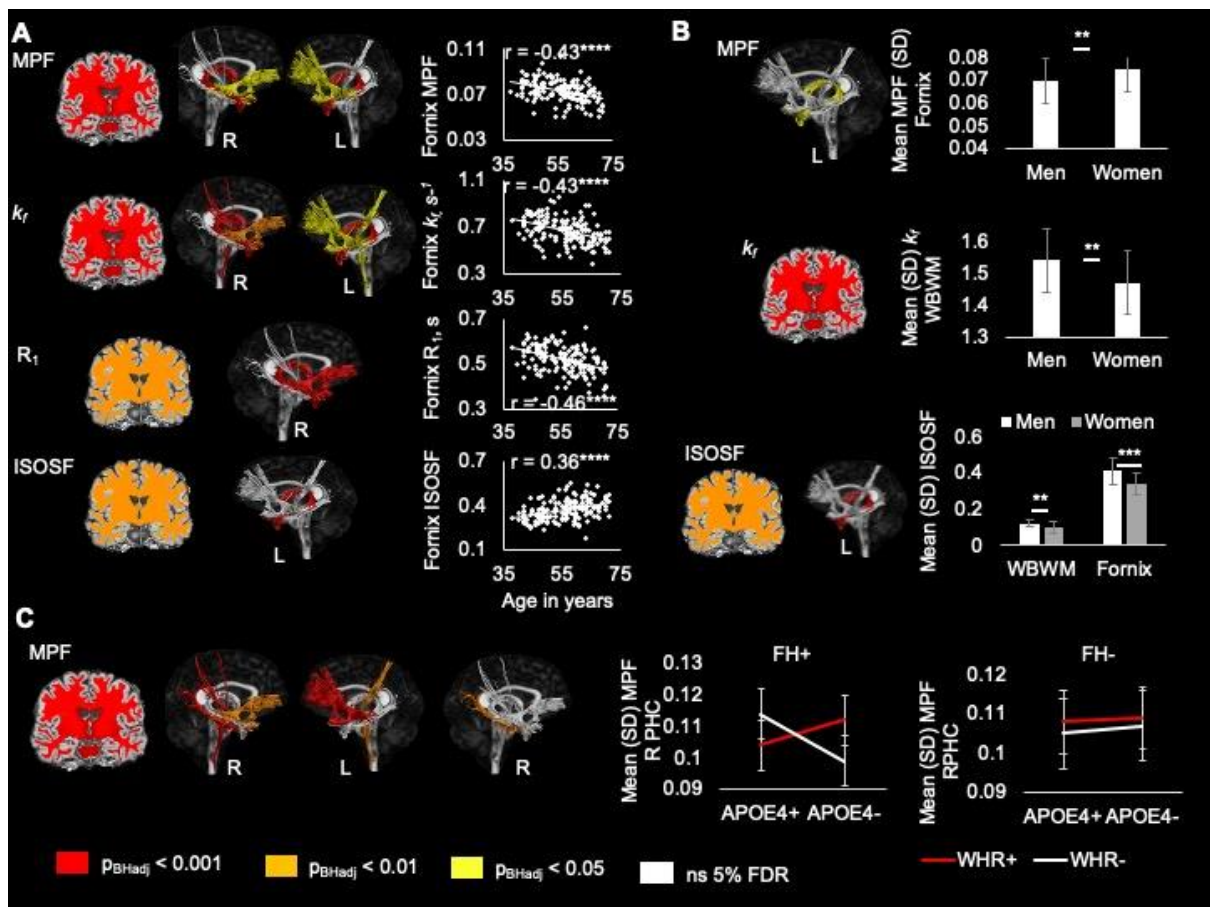
Figure 2 Main effects of age (A) and sex (B) and three-way interaction effect between Family History of dementia (FH), *APOE* genotype and Waist Hip Ratio (WHR) (C) on white matter microstructure colour-coded according to 5% False Discovery Rate (FDR) corrected p-values. Abbreviations: *APOE,* Apolipoprotein E; APOE4+, *APOE*-ε4 carriers (*APOE*-ε2/ε4, *APOE*-ε3/ε4, *APOE*-ε4/ε4); APOE4-, *APOE*-ε4 non-carriers (*APOE*-ε2/ε2, *APOE*-ε2/ε3, *APOE*-ε3/ε3); FH, Family History of dementia; FH+, positive family history; FH-, negative family history; ICSF, intracellular signal fraction; ISOSF, isotropic signal fraction; L, left; MPF, macromolecular proton fraction; p_{BHadj}, p-value corrected for multiple comparison with 5% FDR using the Benjamini-Hochberg adjustement; R, right; R_1, longitudinal relaxation rate; PHC, parahippocampal cingulum; WHR, Waist Hip Ratio; WHR+, centrally obese; WHR-, WHR in normal range.